Clays and Clay Minerals, Vol. 67, No. 6:518–536, 2019

ON THE THERMODYNAMIC STABILITY OF ILLITE AND I-S MINERALS

Stephen U. Aja*

Department of Earth and Environmental Sciences, Brooklyn College and The Graduate Center, City University of New York, 2900 Bedford Avenue, Brooklyn, NY 11210-2889, USA

Abstract—A review of the models proffered to advance the notion of the metastability of illite shows that these models are not supported by the various data groups that have become available. Given that clay minerals are products of water–rock interactions, low-temperature hydrothermal experiments provide singular insights into their relative stabilities; such experiments with natural materials of contrasting pedigree (illites, sericites, muscovites, and chlorites) show that clay-mineral behaviors in low-temperature hydrothermal solutions are amenable to equilibrium thermodynamic conventions. The data from hydrothermal experiments coupled with data from geothermal fields indicate that muscovite is not a stable phase in the *P-T-X* range in which authigenic illite occurs; given that experimental data and field occurrence suggest that muscovite and illite have different *P-T* stability regimes, the continued use of muscovite as a proxy for illite in thermodynamic models is of questionable utility. Furthermore, morphometric studies of clays undergoing illitization show that crystal-size distributions exhibit log-normal patterns. Because log-normal distributions derive from maximum entropy effects, these crystal-size distributions may reflect the effects of entropy production during crystallization rather than kinetically driven Ostwald ripening of illitic phases; the small crystal size of clay minerals may derive from constraints imposed by the physicochemical conditions of their environments of formation. Presumably, irreversible thermodynamics provides the framework for a quantitative understanding of the evolution of complex clay minerals in space and time.

Keywords—Clay-mineral solubility · Entropy production · Illite stability · Metastability · Ostwald process

INTRODUCTION

Illite and mixed-layered illite-smectites (I-S) are the most abundant clay minerals in the Earth's crust; they comprise ~40% of the modal mineralogy of sedimentary rocks and also form common constituents of hydrothermally altered rocks. Clay-mineral diagenesis may be characterized by smectite illitization reactions in which smectite transforms to illite through the development of a series of mixed-layered I-S phases; i.e.:

Smectite→random mixed-layered I-S→
ordered mixed-layered I-S→illite

Illitization reactions have been documented during burial diagenesis of argillaceous sediments (Dunoyer de Segonzac 1970; Perry & Hower 1970; van Moort 1971; Foscolos & Kodama 1974; Heling 1974; Hower et al. 1976; Boles & Franks 1979), hydrothermal alteration of volcanic deposits (Inoue et al. 1978; Inoue & Utada 1983), alteration of sediments in geothermal environments (Muffler & White 1969; McDowell & Elders 1980; Lonker et al. 1990), and contact metamorphism of shales (Nadeau & Reynolds Jr 1981; Pytte & Reynolds 1989; Drits et al. 2007). In earlier investigations, K-fixation (Hower et al. 1976; Eberl & Hower 1977), selective cannibalization of smectite layers of I-S (Pollastro 1985), smectite dissolution, and concomitant crystallization of illite (Ahn & Peacor 1986; Dong & Peacor 1996) have been evaluated as possible factors governing illitization reactions. The illitization reaction becomes detectable at temperatures higher than surface temperatures (50°C, Perry & Hower 1970) and the estimated temperature for the development of zero expandable illite varies from 200 to 264°C (Steiner 1968; Inoue et al. 1978; McDowell & Elders 1980; Inoue & Utada 1983) and underscores that factors besides temperature, such as the composition of coexisting pore fluids (Roberson & Lahann 1981; Inoue 1983), determine the extent of smectite illitization in a particular setting. In addition, in some geothermal and/or hydrothermally altered assemblages, smectite, ordered I-S, and illite crystallized directly from hydrothermal solutions without undergoing the stepwise transformation typical of illitization reactions (e.g. Tillick et al. 2001).

The mineralogical and geochemical consequences of the particular mechanisms by which illitization may occur (solid-state transformation, dissolution and crystallization, and Ostwald ripening) have been evaluated by Altaner & Ylagan (1997); in their analyses, those authors concluded that Ostwald ripening describes illitization rather poorly owing to the progressive mineralogical and chemical changes during illitization. They further concluded that a solid-state transformation mechanism models illitization in rock-dominated systems such as bentonite whereas a dissolution and crystallization mechanism applies to fluid-dominated systems typified by sandstones and hydrothermal environments; ostensibly, both mechanisms may occur in shales, and permeability may explain the differences in reaction mechanism. In other words, both solid state transformation and dissolution-crystallization take place in a fluid medium though the former occurs under a more limited supply of fluids. Both mechanisms may thus simply be expressions of the effect of variable fluid/rock ratios on the same neoformation process.

* E-mail address of corresponding author: suaja@brooklyn.cuny.edu
DOI: 10.1007/s42860-019-00044-x

Illitization reactions have also been shown to be catalyzed by microbial mineral reactions (Kim et al. 2004, 2019; Zhang et al. 2007; Jaisi et al. 2011). Kim et al. (2004) effected the conversion of smectite to illite by incubating a dissimilatory metal-reducing bacterium (*Shewanella oneidensis* strain MR-I) with nontronite for 14 days at 1 atmosphere; the reduction of structural trivalent iron by the microbes promoted the dissolution of the Fe-rich smectite and subsequent neoformation of an illite. In a test of the idea that the smectite-to-illite reaction can be promoted by bacteria in the presence of organic matter, Zhang et al. (2007) demonstrated that bioreduction of Fe(III) in Fe-rich smectites owing to intercalated organic matter may promote illitization in some instances (e.g. cysteine-intercalated nontronite) whereas in other instances (e.g. toluene-intercalated nontronite) intercalated organic matter does not promote illitization; in the former case, the catalytic consequences of bioreduction concurred with the notion of a dramatic reduction in the required geologic time and elevated temperature. Jaisi et al. (2011) studied the effects of a variety of factors (pH, temperature, solution chemistry, and aging) on a microbially mediated smectite illitization reaction, and thus further confirmed that the formation of illite during smectite-to-illite reaction may be catalyzed by bioreduction, and this depresses the temperature and time normally required for illitization by inorganic geochemical processes. In a natural analogue investigation of microbially mediated illitization, Kim et al. (2019) studied sediments from the International Ocean Discovery Program (IODP) Site C0023, Nankai Trough, offshore Japan; they concluded that illite abundance in the deepest sediment (700–1300 m) is consistent with abiotic burial diagenesis whereas diagenetic alterations in the intermediate zone (400–700 m) may have resulted from a microbially induced smectite-to-illite transition by means of biotic reduction of phyllosilicate structural Fe(III) in clays of the IODP mudstones.

The illitization of smectite through mixed-layered I-S has been viewed as an application of Ostwald's step rule (Morse & Casey 1988); i.e., "If a reaction can result in several products, it is not the stablest state with the least amount of free energy that is initially obtained, but the least stable one, lying nearest to the original state in free energy" (Ostwald 1897). Clay-mineral formation and paragenesis have, thus, been thought to follow the Ostwald step rule and ripening processes, though they tend to form more ordered or complex structures (compared to carbonates and oxides) with time (Morse & Casey 1988). The Ostwald step rule implies that mineral paragenetic pathways may proceed via thermodynamically unfavored phases and thus clay diagenetic transformations may reflect a disequilibrium process controlled by relative rates. Ordinarily, the operation of the step rule would reflect the kinetic advantages of forming metastable intermediates relative to the comparative rate of forming the stable phases directly. Nonetheless, the Ostwald step rule is simply a qualitative description of empirical observation (e.g. Chung et al. 2009) and does not provide a rigorous thermodynamic and, hence, predictive model of mineral behavior. Clearly, the question is still largely unresolved as to whether the treatment of clay-mineral paragenesis in low-temperature environments should adopt kinetic formalisms rather than equilibrium thermodynamic approaches. The development of an accurate model of the thermodynamic status of smectite, I-S, and illite serves crucial heuristic and practical purposes; in this discussion, the question of the stability or metastability of these clay minerals will be reassessed in light of recent structural and experimental thermodynamic data.

ILLITIZATION AND OSTWALD PROCESSES

Ostwald ripening (or coarsening) is undergone by metallic and non-metallic systems and describes a phase-transformation process following nucleation in a given medium containing particles with various sizes. Such an ensemble of nucleated particles does not represent a minimum energy configuration owing to the excess surface energy present in the system. To achieve thermodynamic equilibrium, surface-energy minimization is achieved by the growth of large particles with a concomitant dissolution of smaller particles; the total energy of the system is, thus, decreased by the interfacial energy-driven mass transfer. In a closed system, the surface-energy minimization reaches a theoretical endpoint when a single crystal containing the entire volume fraction of the growing phase forms. Also, morphological changes may occur owing to the dissolution of the small particles and subsequent transfer of their mass to the larger particles. The theoretical underpinning of Ostwald ripening, provided by Lifshitz & Sloyozov (1961) and Wagner (1961) (the LSW theory), made quantitative predictions on the long-time behavior of coarsening systems by assuming that the coarsening rate of a particle is independent of its surroundings; hence, at long times the cube of the average particle radius should vary linearly with time, and when scaled by the average radius, the particle radii should assume a time-independent form (see discussions in Baldan 2002). However, the time-independent distribution of radii predicted by LSW is usually not observed experimentally. Because Ostwald ripening has been presumed to be the basic process of aggrading neomorphism (Morse & Casey 1988 and references therein), several studies of morphological and crystal-size distributions of illite and I-S clay minerals samples from a variety of geological settings have been reported in the literature.

Morphometry of Illite and I-S Crystallites

The implications of recent morphometric studies (Eberl & Środoń 1988; Inoue et al. 1988; Lanson & Champion 1991; Eberl et al. 1990, 1998; Inoue & Kitagawa 1994; Środoń et al. 2000) for illite stability and for illitization mechanism are somewhat unresolved. The sericites from the Silverton caldera (Colorado), formed by hydrothermal alteration, exhibited a linear relation between apparent K-Ar age and maximum expandability of the sericites which was attributed to Ostwald ripening of an older clay during a later hydrothermal event (Eberl & Środoń 1988); the shape of the steady-state profiles of the reduced coordinates of the grain-size distribution histograms appeared indicative of Ostwald ripening in a closed system. The maximum size of the steady-state profiles and the general shape of the profiles, however, do not match any of the theoretically calculated profiles, and an inverse correlation between maximum expandability and fixed interlayer charge (K + Na) per half unit

https://doi.org/10.1007/s42860-019-00044-x Published online by Cambridge University Press

cell was also documented, which is indicative of chemical changes during the hydrothermal alteration of the sericites.

Crystal-size analyses have also been reported in a study of the applicability of Ostwald ripening to I-S reactions for a series of I-S minerals from the Shinzan (Japan) hydrothermal area (Inoue et al. 1988). That study focused on the illite-growth mechanism during illitization of I-S clay having 50–0% expandable layers because of the presumption that short- and long-range ordered I-S grains with 50–0% expandable layers are immature illites undergoing growth; the K content per half unit cell for the samples investigated varied from 0.29±0.07 (55±5% expandable) to 0.80 ± 0.01 (0% expandable). They deduced that grain-length and grain-width histograms vary systematically as functions of percent expandable layers, and the length and width distributions normalized to the modes give steady-state profiles. These observations were interpreted to mean that the Ostwald ripening process governed the coarsening in the lateral faces of I-S particles and that the shape of steady-state profiles demonstrated that the growth of the I-S minerals is dominated by a spiral-growth mechanism inasmuch as Ostwald ripening theory predicts a steady state profile when a grain-size histogram is plotted in reduced coordinates. Hence, the same Ostwald ripening mechanism can be used to describe growth of both the lath-shaped particles (55–20% expandable I-S) and the hexagonal shaped particles (20–0% expandable I-S) (Inoue et al. 1988). As was the case for the Silverton sericites, the samples studied underwent compositional changes (as indicated by $K_x/O_{10}(OH)_2$).

In further morphological studies of smectite illitization owing to Miocene Kuroko ore mineralization, Inoue & Kitagawa (1994) investigated I-S and illite from the Kamikita hydrothermal alteration area (Japan); for the samples studied, expandable layers varied from 12 to 0%. The reduced size coordinates yielded steady-state profiles that were independent of the formation ages and temperatures, and also skewed towards larger values for particle-size distribution. The steady-state profiles of the normalized distribution of particle diameter and particle thickness were deemed to be consistent with the Ostwald ripening mechanism during the late stages of illitization. Moreover, the growth spirals occurred most commonly on the basal surfaces of illite crystals, which they interpreted to mean that spiral growth was the growth-controlling mechanism for the Ostwald ripening during the late stages of illitization; also, the normalized particle-size distribution curves fitted better to a log-normal distribution curve than to the theoretical profile calculated for a screw-dislocation (Inoue & Kitagawa 1994).

Clay samples from the late-stage burial diagenetic alteration of smectite to illite (i.e. ordered mixed-layered I-S → illite) sequence of the Paris Basin were studied by Lanson & Champion (1991). They documented the existence of two particle populations including an illitic phase that changes little with depth and an I-S phase that becomes less smectitic with depth. Particle sizes for the illitic samples (whole samples, lath-shaped, and hexagonal-shaped) plotted as reduced coordinates skew to larger sizes as is expected for dynamic crystal growth typical of the Ostwald ripening mechanism. However, the normalized modes of the grain-size distribution fit log-normal distributions and, moreover, Ostwald ripening is strictly applicable to a monomineralic closed system, constraints which are not satisfied in those studies (Lanson & Champion 1991).

The universality of the log-normal distribution of crystal-size distributions of illite fundamental-particle thicknesses was further validated by Środoń et al. (2000) using samples collected from several bentonites and hydrothermally altered volcanics (Upper Silesia Coal Basin Carboniferous bentonite, Welsh Borderlands Silurian bentonite, hydrothermally altered Silverton caldera sericites, hydrothermally altered rhyolite from Zempleni Hills (Hungary), East Slovak basin Miocene bentonite, hydrothermally altered volcanics from Central Slovakia, and hydrothermally altered Miocene volcanics from Japan). Furthermore, those authors concluded that the three-dimensional crystal-growth characteristic of the latter stages of illitization cannot be explained by Ostwald ripening, supply-controlled crystal growth, or the coalescence of smectite layers and that these crystal-growth mechanisms do not explain the observed evolution of the mean and variance of the crystal dimensions and the observed shapes of crystal-thickness distributions. On the whole, crystal-size distributions of illitic and I-S samples from bentonites, hydrothermal altered volcanic rocks, and burial diagenetic sequences have been shown by the various studies to be log-normal distributions.

The probability density function of a log-normal distribution of the variable X conforms to the model (Eberl et al. 1998; Środoń et al. 2000):

$$g(X) = \left[\frac{1}{X\beta\sqrt{2\pi}}\right]\exp\left\{-\frac{[\ln(X)-\alpha]^2}{2\beta^2}\right\} \quad (1)$$

If X is the crystal dimension and f(X) is the observed frequency of the crystal dimension, then the mean of the logarithm of the crystal dimension (α) and the variance of the crystal dimension (β) are given by the following:

$$\alpha = \int \ln(X) f(X) \quad (2)$$

$$\beta^2 = \int [\ln(X)-\alpha]^2 f(X) \quad (3)$$

Moreover, a log-normal distribution of crystal-size distribution reflects crystal growth predicated on size-dependent growth and results from the operation of the Law of Proportionate Effect, given as (Eberl et al. 1998):

$$X_{j+1} = X_j + \epsilon_j X_j \quad (4)$$

where X_j is the initial crystal size parameter, X_{j+1} is the new crystal-size parameter after one growth cycle, and ϵ_j is a random varied number (with value between 0 and 1) that measures the system's variability. Implicit in the factor of system variability are the effects of the geological environment, the thermodynamic properties of the minerals, and petrophysical constraints on the crystal-growth processes.

https://doi.org/10.1007/s42860-019-00044-x Published online by Cambridge University Press

The effect of system variability on clay-mineral growth and stability, implicit in the operation of the law of proportionate effect, probably translates into the question of the effect of the rate of entropy production on clay-mineral neoformation and stability.

Entropy Production and Crystal-size Distributions

In general, log-normal distributions reflect the cumulative product of a variable influenced by many small independent factors and are indicative of the multiplicity of factors in the illite growth mechanism during illitization; their characteristic skew apparently arises from the non-linear fluctuations in successive reaction steps and, hence, the utility of the law of proportionate effect in reproducing log-normal distributions of crystal sizes. Because skewed distributions are common when variance is large, log-normal distributions apparently derive from the increasing entropy of equilibrium distributions of natural processes of growth. In other words, log-normal distribution is the maximum entropy probability distribution for a random variable X for which the mean (see Eq. 2) and variance (see Eq. 3) of ln(X) are specified (Berrill & Davis 1980; Groṅholm & Annila 2007). The principle of maximum entropy is rooted in the second law of thermodynamics and applies when non-uniformity of outcomes (in this case crystal growth) is expected and provides that as a physical system evolves toward equilibrium its entropy is increasing. For heterogeneous systems undergoing reactions in which chemical reactions are distributing matter among various chemical compounds, the total probability of the interactions quantifies the entropy; i.e., $S = \mathrm{R}\ln P$ where P is the overall probability. For such a heterogeneous system containing a total number of reacting atomic constituents, N_j, the entropy in the system (Sharma & Annila 2007) is:

$$S = \frac{1}{T}\sum_{j=1} N_j\left(A_j + \mathrm{R}T\right) \tag{5}$$

where S is the entropy, T denotes absolute temperature, R is the universal gas constant, and A_j is chemical affinity. The time derivative of Eq. 5 is the rate of entropy production (Sharma & Annila 2007); i.e.

$$\frac{\mathrm{d}S}{\mathrm{d}t} = \frac{1}{T}\sum_{j=1} \nu_j A_j \geq 0 \tag{6}$$

The rate of entropy production (Eq. 6) embodies the exchange of entropy and matter with the surroundings and also the rate of entropy production due to irreversible processes associated with the various reactions. Thus, the log-normal distributions may derive from the increasing entropy of equilibrium distributions of natural processes of growth inclusive of the effect of system variability on the growing crystals.

CRYSTAL SIZE AND STABILITY OF CLAY MINERALS

The small size of clay minerals in surface and near-surface environments has been held to reflect details of their crystal structure rather than the temperature and pressure conditions at which they formed (Meunier 2006). In his excellent review article, Meunier (2006) reasoned that genetic models for the small crystal sizes of clay minerals and the allomorphic shape of some clay minerals derive from the effect of order-disorder on the crystal-growth processes of clay minerals. Clay-mineral structures contain various scales of disorder which are expressed ultimately as structural defects. These structural defects include defects in the c direction, which may arise from faults in stacking layers of constant thickness or from stacking layers of variable thickness which gives rise to mixed layers. In addition, crystal defects inside the 2:1 layer may arise from order-disorder within the tetrahedral sheets, order-disorder in dioctahedral sheets, and order-disorder in the interlayer zone. Within the framework of periodic bond chains (Hartman 1973), Meunier (2006) speculated that the state of order affects the development of the periodic bond chain (PBC). A random distribution of interlayer cations leads to development of zero PBC and, hence, favors small montmorillonite crystallites. In contrast, incorporation of ordered interlayer cations (in beidellite, vermiculite, and illite) imply the existence of up to 3 PBCs and, hence, the development of euhedral crystallites. Meunier (2006) further speculated that the presence of numerous crystal defects hinders the growth of nucleated crystallites; thus, in the low-temperature conditions ($T \leq 250$°C) of clay genesis, nucleation is always favored over crystal growth, leading to the characteristic small size of clay minerals.

An alternative model, however, is that the small size of clay minerals is a function of the temperature and pressure conditions at which they grow and reflects constraints present during growth. Illitization reactions are driven by increasing temperatures and, given that entropy production drives chemical reactions that occur in response to heating effects (Loucks 1991), illite formation and stability may be impacted significantly by the rate of entropy production. Within the context of irreversible thermodynamics, entropy production per unit time in an isolated system may be given (Prigogine 1961) as:

$$\frac{\mathrm{d}S}{\mathrm{d}t} = \frac{1}{T}\sum_{p} A_p \nu_p > 0 \tag{7}$$

where $\frac{\mathrm{d}S}{\mathrm{d}t}$ is the rate of entropy production owing to changes in the system, A_p is the chemical affinity of the p^{th} reaction which is linked to the chemical potential of the reacting species and vanishes at equilibrium, $\nu_p\left(=\frac{\mathrm{d}\xi_p}{\mathrm{d}t}\right)$ is the reaction velocity or the rate of change of the progress variable of the p^{th} reaction, and T is the absolute temperature. The rate of entropy production is an inverse function of temperature (Eq. 7) and, thus, entropy production for illitic phases formed during prograde illitization will diminish with increasing temperatures of illitization up to the stability limit of illite; by contrast, entropy production is likely to be a less significant factor in the formation and stability of macroscopic mica (being higher temperature phases) relative to illite. One aspect of entropy production during the crystallization of the illitic phases may derive partly from the entropic contribution of structural water to the

https://doi.org/10.1007/s42860-019-00044-x Published online by Cambridge University Press

intermolecular bond energy and may be amplified by the variable states of structurally bound water in illites and I-S phases.

Effects of Bound Interlayer Water

The molar proportion of structurally bound H_2O [$H_2O(+)$] as a function of the molar proportion of interlayer cations was evaluated by Loucks (1991) based on 72 wet-chemical analyses of muscovite, lepidolite, and illite from igneous, metamorphic, low-pressure hydrothermal, and sedimentary environments; he presumed the limiting substitutions:

$$(H_3O^+)Al_2AlSi_3O_{10}(OH)_2 \leftrightharpoons KAl_2AlSi_3O_{10}(OH)_2$$
$$(H_2O)Al_2Si_4O_{10}(OH)_2 \leftrightharpoons KAl_2AlSi_3O_{10}(OH)_2 \text{ and}$$
$$Al_2Si_4O_{10}(OH)_2 \leftrightharpoons KAl_2AlSi_3O_{10}(OH)_2$$

His analysis demonstrated that the total structural H_2O contents may be predicted by assuming that the interlayer may contain both neutral water molecules and hydronium ions, $(H_3O)^+$, associable with hydropyrophyllite [$(H_2O)Al_2Si_4O_{10}(OH)_2$] and hydromica [$(H_3O^+)Al_2AlSi_3O_{10}(OH)_2$] components, respectively. On average, the hydromica substitution $(H_3O)K_{-1}$ accounts for 73% of interlayer H_2O in the sample group, whereas the hydropyrophyllite substitution $H_2OSi(KAl)_{-1}$ accounts for only 27% of the interlayer H_2O in the average muscovite. However, because of the sparsity of high-quality analytical data, the analyses included only five illitic samples, and this raises the question whether the contribution of the $Al_2Si_4O_{10}(OH)_2 \leftrightharpoons KAl_2AlSi_3O_{10}(OH)_2$ substitution to the compositional trend might be greater. Nonetheless, the systematic variation in white mica H_2O content is amenable to a crystal-chemical model that considers all interlayer sites to be occupied by alkali and alkaline earth cations, hydronium ions, and H_2O molecules. In terms of the various thermal regimes covered by the study of Loucks (1991), structurally bound water in illitic phases from low-temperature sedimentary environments have both more variation in the amounts of structural water and substantially larger mean values compared to micas from hydrothermal and metamorphic environments. Water in igneous and high-grade metamorphic micas approximates the stoichiometric OH-halogen allotments and are also the least amount of water in these phases.

The variable states of structurally bound water would probably contribute to the Gibbs free energy of crystallization of illitic phases such that (cf. Yau et al. 2000):

$$\Delta G^{o}_{cryst} = \Delta H^{o}_{bond} - T\Delta S^{o}_{bond} - T\Delta S^{o}_{H_2O(+)} \quad (8)$$

The notion that the variable states of structural water enhance significantly the stability of illitic phases (Loucks 1991) is consistent with the understanding that the structuring of water molecules is an important thermodynamic driver of crystallization (De Yoreo & Vekilov 2003).

A THERMODYNAMIC MODEL OF CLAY-MINERAL BEHAVIOR

Clay minerals are hydrous phases the formation of which results from water–rock interactions in surface and near-surface environments. Consequently, solubility techniques (either solution equilibration or solubility sensu stricto) provide a unique way to assess directly the thermodynamic behaviors of minerals in this mineral group. Experimental determination of the stability of clay minerals faces challenges peculiar to the low-temperature regimes of their occurrences (see review by Manning 2003), and the demonstration of the attainment of equilibrium in solubility measurements has been a particularly vexing question. Numerous solubility studies have been reported in the literature for various clay minerals and, in some of the earliest studies (e.g. Reesman & Keller 1968; Routson & Kittrick 1971), the attainment of equilibrium was not demonstrated affirmatively; rather equilibrium was presumed and the identity of the solubility-controlling phases was not ascertained directly. The bulk compositions of the starting natural clays were, thus, wrongly presumed to be the same as the composition of the solubility-controlling phases and, moreover, ion speciation analyses of the reacted solutions were generally omitted. Owing to these earlier shortcomings, recent reviews of the clay-solubility literature have tended to be generally dismissive of all solubility studies regardless of whatever adaptations had been undertaken in later studies to correct deficiencies of the earlier studies, thus necessitating some further clarifications.

Solution Equilibration Investigations

Experimental investigations of the thermodynamic stability of natural illites are constrained by the rarity of single-phase, monomineralic reference or standard illite samples. X-ray powder diffraction surveys of ordered illite-smectites and illitic (or illite-like clay containing some expandable layers) materials from mostly diagenetic environments demonstrated that discrete illite is commonly intermixed with ordered illite-smectite in reference illites; e.g. Fithian illite, Beavers Bend illite, Marblehead illite, and Silver Hill illite have been shown to be I+ISII mixtures (Środoń 1984; Środoń & Eberl 1984). In a long-term (up to 2.6 years) solubility experiment with Goose Lake, Beavers Bend, and Fithian illites at 25°C, Kittrick (1984) concluded that natural illites contain two or more clay phases or components in equilibrium with each other; this deduction, based on solubility measurements, is thus consistent with the prior determination by Środoń (1984) that the reference illites are multiphase mixtures. The peculiar problem posed by these intermixtures derives from the impossibility of mechanical separation of these clay phases; incidentally, recent studies with natural reference illites (e.g. Nieto et al. 2010; Gailhanou et al. 2012; Smith et al. 2017) seem to have presumed that these reference or standard illites are single-phase, micaceous materials when in fact they are mixtures. In this context, treating these natural samples as single-phase, micaceous materials is likely to yield ambiguous results. Solution equilibration techniques provide an approach to resolving the solubility and

https://doi.org/10.1007/s42860-019-00044-x Published online by Cambridge University Press

thermodynamic stability of the component phases in such clay minerals. The equilibration of solid assemblages with aqueous compositions of variable initial compositions can bring some of the component phases to equilibrium and, as the experimental temperature is varied, the thermal evolution of the solubility-controlling mica-like phases becomes apparent. Thus, the basic experimental strategy in solution equilibration investigations is to bring the component phases of natural illite to equilibrium in a manner that facilitates demonstration of equilibrium by the analysis of the equilibrated solutions.

Solution equilibration studies of illites Several natural illites, including Goose lake illite (GL), Beavers Bend illite (BB), Silver Hill illite (SH), and Marblehead illite (MH) (Table 1), were utilized in a series of solution equilibration experiments (Rosenberg et al. 1985; Sass et al. 1987; Aja 1991; Aja et al. 1991a, 1991b; Aja & Rosenberg 1996).

The Goose Lake illite (Goose Lake, Illinois) is a Pennsylvanian underclay and was originally characterized by Grim & Bradley (1939) as a non-bentonitic illite containing small amounts of quartz, kaolinite, and organic matter; it (GL) is a mixed-layered illite with expandability between 25 and 30% (Gaudette et al. 1966a, 1966b). Fithian illite is a Pennsylvanian underclay from Vermillion County, Illinois (Grim et al. 1937; Gaudette et al. 1966a, 1966b). The Beavers Bend illite is a well crystallized illite from an unweathered claystone from the Silurian Blaylock Formation in the Ouachita Mountains (Beavers Bend State Park of southeastern Oklahoma); some samples contain minor chlorite as a mechanical mixture (Mankin & Dodd 1963; Gaudette et al. 1966a, 1966b). Silver Hill illite derives from a Cambrian shale in Montana (Hower & Mowatt 1966), has a modal mineralogy of 89% illite-smectite content (Kuila & Prasad 2013), and <10% expandable layers (Hower & Mowatt 1966). The Marblehead illite is a pure, well crystallized $2M_1$ illite, has <5% mixed-layering, and occurs as large pockets of gray laminated clay in Silurian dolomite (Burnt Bluff Group) near Marblehead, Wisconsin (Gaudette 1965; Gaudette et al. 1966a, 1966b). Güven (1972) also reported the presence of trigonally arranged twin aggregates in MH and suggested its derivation from a phengitic mica. The presence of varying amounts of expandable layers in BB, SH, MH, and GL is indicated by the CEC (meq/100 g) of 18.48, 15, 21.18, and 24.20, respectively (Gaudette et al. 1966b; Hower & Mowatt 1966); furthermore, BB, SH, and MH have been shown to be mixtures of discrete illite and ISII (see Table 1). Clearly, these natural samples are of divergent geological pedigrees and have varying amount of expandable components and quite different bulk chemistries.

In the experiments with these natural illites, illite chemical compositions were, in the first instance, projected onto the quaternary system, K_2O-Al_2O_3-SiO_2-H_2O; in this system, three solid phases can be in equilibrium with solution at a given temperature and pressure. Hence, KCl solutions were reacted with mixtures of illite and two other solids (kaolinite-gibbsite, kaolinite or microcline plus quartz or Cab-O-Sil) from 25 to 250°C. In order to bring solutions to equilibrium rapidly, starting solutions (0.2 M and 2.0 M KCl/HCl or KCl/KOH) were equilibrated with approximately equal weights of the mineral mixtures. The experiments were conducted in pairs with identical solid mixtures and solutions having the same ionic strength but with high and low values of K^+/H^+. Under isothermal and isobaric conditions, the mineral mixtures will control pH, pK^+, and $pSiO_{2(aq)}$ if Al is conserved. The attainment of equilibrium was generally based on the reversibility of a_{K^+}/a_{H^+} ratios in solutions; equilibrium was approached from silica undersaturation in most of the experiments, but reversibility of $a_{SiO_{2(aq)}}$ was demonstrated by approaching equilibrium from silica supersaturation in some experiments. At the conclusion of each experiment, the solid products were separated from the equilibrated solutions by immiscible displacement techniques; the solid products were characterized by X-ray diffractometry while the solutions were analyzed using conventional wet chemical techniques (additional details of experimental and analytical procedures are available in Sass et al. 1987 and Aja et al. 1991a). The molalities of the quench solutions were corrected to activities at temperature using the Pitzer phenomenology (Aja 1989 and references therein); the resulting ion activities were then plotted in ion activity diagrams (Fig. 1).

If the component phases in the illites behaved as a solid solution under isothermal and isobaric conditions, the solubility data should fit onto a single curvilinear pattern. This was not the case (fig. 1 in Aja et al. 1991a); rather, the solubility data from the solution equilibration experiments have linear dispositions. At 25 and 60°C, for instance, data in experiments with MH (Fig. 1a, b) and GL (Fig. 1c) show negatively sloping lines as expected for kaolinite–illite phase boundaries for illites of fixed compositions. Under isothermal and isobaric conditions, the solubility data show multiphase solubility patterns which are consistent with these reference illites being multiphase mixtures. These solubility data also imply the existence of a large group of particles having a similar chemical composition and physical state. In order to determine the K-contents of the mica-like solubility-controlling phases from the univariant boundaries, the phases were presumed to have the general structural formula, $K_x(Al_2)(Al_xSi_{4-x})O_{10}(OH)_2$. The univariant kaolinite ⇌ illite reaction is,

$$K_x(Al_2)(Al_xSi_{4-x})O_{10}(OH)_2 + xH^+_{(aq)} + \left(1+\frac{x}{2}\right)H_2O \rightleftharpoons \frac{2+x}{2}\,Al_2Si_2O_5(OH)_4 + xK^+_{(aq)} + (2-2x)SiO_{2(aq)} \quad (9)$$

Applying the law of mass action leads to

$$\log\frac{a_{K^+}}{a_{H^+}} = \frac{2x-2}{x}\log a_{SiO_{2(aq)}} + \frac{1}{x}\log K_9 \quad (10)$$

Equation 10 is the equation of a straight line the slope of which is a function of x or the K-content per half unit cell of the solubility-controlling phases. From the slopes of the plots of $\log\frac{a_{K^+}}{a_{H^+}}$ vs $\log a_{SiO_{2(aq)}}$, values for $K_x/O_{10}(OH)_2$ were determined to be 0.29 ± 0.04, 0.50 ± 0.05, 0.69 ± 0.08, and 0.85 ± 0.05 (Fig. 2; also Table 1 in Aja et al. 1991a). The relative stabilities

https://doi.org/10.1007/s42860-019-00044-x Published online by Cambridge University Press

Table 1 Bulk compositions of natural samples used in solution equilibration studies

Beavers Bend illite	$K_{0.53}(Al_{1.66}Fe_{0.20}Mg_{0.13})(Si_{3.62}Al_{0.39})O_{10}(OH)_2$	I+ISII*
Goose lake illite	$K_{0.59}(Al_{1.58}Fe_{0.24}Mg_{0.15})(Si_{3.65}Al_{0.35})O_{10}(OH)_2$	
Marblehead illite	$(K_{0.79}Na_{0.02})\left(Al_{1.43}Fe^{+3}_{0.11}Mg_{0.37}Ti_{0.08}\right)(Si_{3.55}Al_{0.45})O_{10}(OH)_2$	I+ISII*
Silver Hill illite	$(K_{0.72}Na_{0.03}Ca_{0.03})(Al_{1.38}Fe_{0.38}Mg_{0.25})(Si_{3.40}Al_{0.60})O_{10}(OH)_2$	I+ISII†
RM30 (sericite)	$(K_{0.83}Na_{0.02}Ca_{0.01})(Al_{1.93}Fe_{0.02}Mg_{0.05})(Si_{3.20}Al_{0.80})O_{10}(OH)_2$	
SG4 (sericite)	$(K_{0.83}Na_{0.05})(Al_{1.89}Fe_{0.01}Mg_{0.09})(Si_{3.27}Al_{0.73})O_{10}(OH)_2$	
Brazilian muscovite	$(K_{0.85}Na_{0.08}Ca_{0.01})(Al_{1.87}Fe_{0.08}Mg_{0.05})(Si_{3.08}Al_{0.92})O_{10}(OH)_2$	

The sericites (RM30 and SG4) formed from hydrothermal alteration of fault gouge in Tertiary volcanics in the Silverton caldera (Eberl et al. 1987). Sources of phase components of natural illites: * Środoń (1984); † Środoń & Eberl (1984).

of these phases are determined by temperature and the chemistry of the coexisting aqueous solutions; for instance, only two of these four phases are stable in solutions at equilibrium with quartz (Fig. 3).

The internal consistency of the experimental solubility data, in the studies discussed above, was tested using the compositions of the solubility-controlling phases calculated independently from the slopes of different univariant

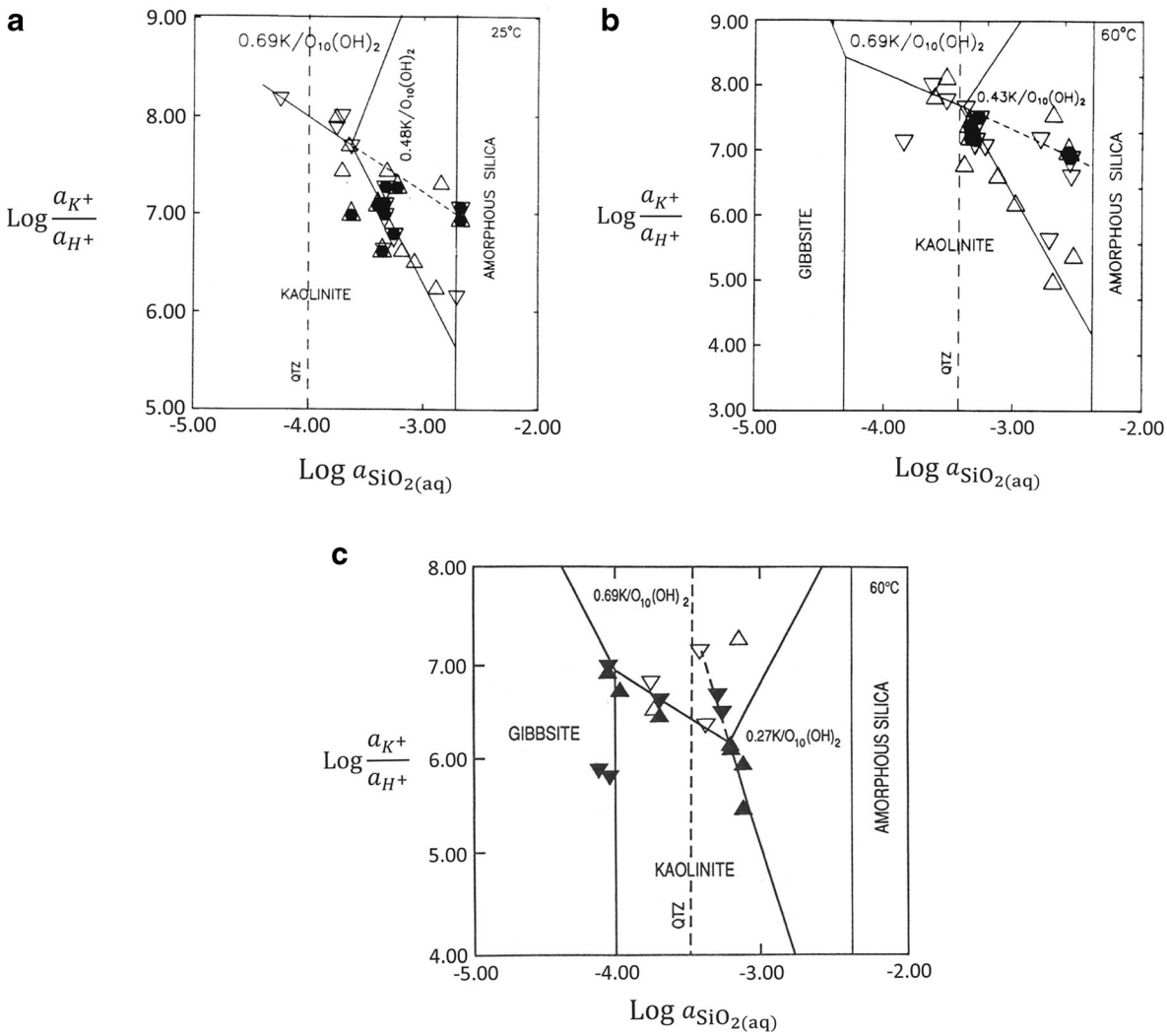

Fig. 1 Solution equilibration data for Marblehead Illite (**a**, **b**) and Goose Lake illite (**c**) depicted on isothermal isobaric activity diagrams. In Figures 1a and 1b, open and partially open triangles indicate experiments in 2 M and 0.2 M KCl solutions, respectively (Aja et al. 1991a). In Fig. 1c, solid triangles and open triangles indicate experimental data for Goose Lake and Beavers Bend illites, respectively (Aja 1991).

https://doi.org/10.1007/s42860-019-00044-x Published online by Cambridge University Press

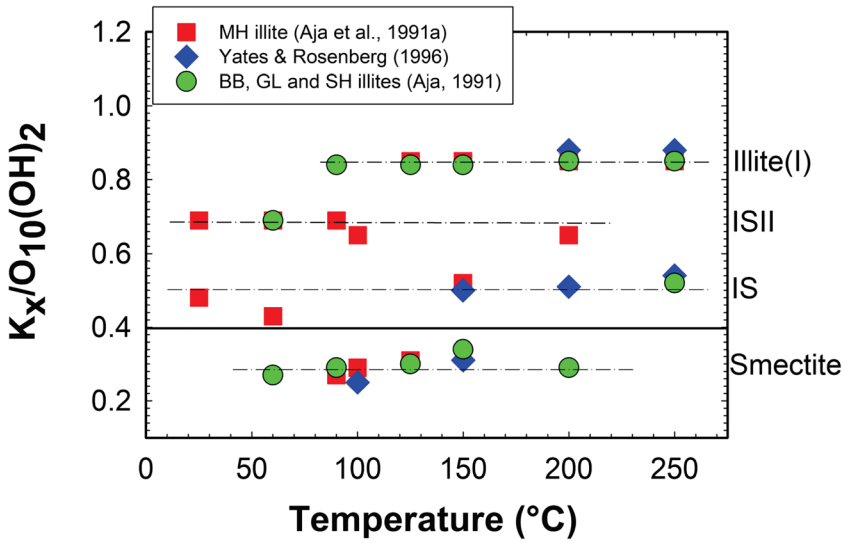

Fig. 2 Variation of the interlayer K-content per half unit cell [$K_x/O_{10}(OH)_2$] of the solubility-controlling phases in the presence of kaolinite between 25 and 250°C; values of the K-content (x) are based on the general structural formula $K_x(Al_2)(Al_xSi_{4-x})O_{10}(OH)_2$ used in the solubility model (Eq. 9). The solid red squares indicate data from experiments with Marblehead illite (Aja et al. 1991a); the solid green circles indicate data reported by Aja (1991) for Beavers Bend, Goose Lake (GL), and Silver Hill (SH) illites; the solid blue diamonds indicate results of solution equilibration experiments with San Juan sericites (RM30, SG4) and Brazilian muscovite (Yates & Rosenberg 1996). Smectite, IS, ISII, and Illite (I) represent the nomenclature of the four mica-like solubility-controlling phases by Rosenberg et al. (1990).

boundaries constraining the stability field of a given illite at a given temperature. For example, Fig. 4 shows the experimental results from the equilibration of illite with either kaolinite or microcline; in the former, additional solid phases included gibbsite or quartz whereas in the latter, the additional phases were quartz or Cab-O-Sil. If the results of the experiments are internally consistent, values of $K_x/O_{10}(OH)_2$ determined independently from the three univariant boundaries containing illite must be in agreement; i.e. values of x calculated from the univariant kaolinite ⇌ illite (x), illite(x) ⇌ gibbsite, and illite(x) ⇌ microcline boundaries must be in agreement if and only if the data are internally consistent. This was demonstrated to be the case for the data plotted in Fig. 4; similar conclusions were reached for experiments conducted at other temperatures. Not only does this conclusion imply that the chemical potential diagrams were topologically consistent, it also strongly implies that equilibrium was attained between illite(x) and the equilibrating solutions. Furthermore, it negates the notion that these experimental observations may derive from adsorption–desorption reactions on surfaces of the illite, especially considering that these experiments were conducted in decade KCl solutions and shows no ionic strength dependence. The

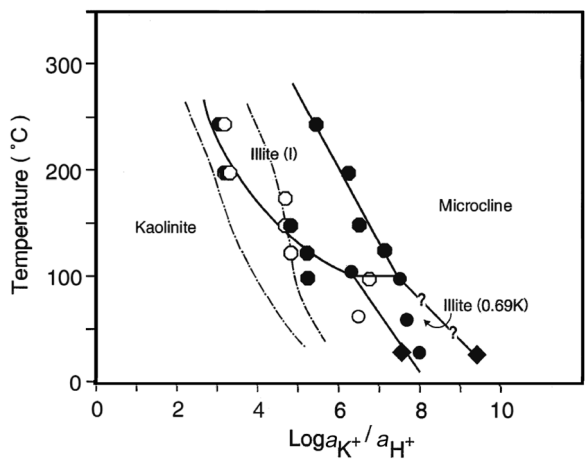

Fig. 3 A depiction of phase relationships in the system K_2O-Al_2O_3-SiO_2-H_2O at quartz saturation using temperature vs $\log\frac{a_{K+}}{a_{H+}}$ coordinates (Aja & Rosenberg 1996). The hexagons and circles represent equilibrium ion activities of phase boundaries with endmember illite [i.e. Illite (I) or illite (0.85K)] and illite (0.69K) [or ISII], respectively. The solid symbols, open symbols and diamonds represent data points from experiments with MH illite, GL illite, and data points from Garrels and Howard (1957), respectively. The dot-dashed boundaries outline the predicted field (Montoya &Hemley 1975) of muscovite stability.

https://doi.org/10.1007/s42860-019-00044-x Published online by Cambridge University Press

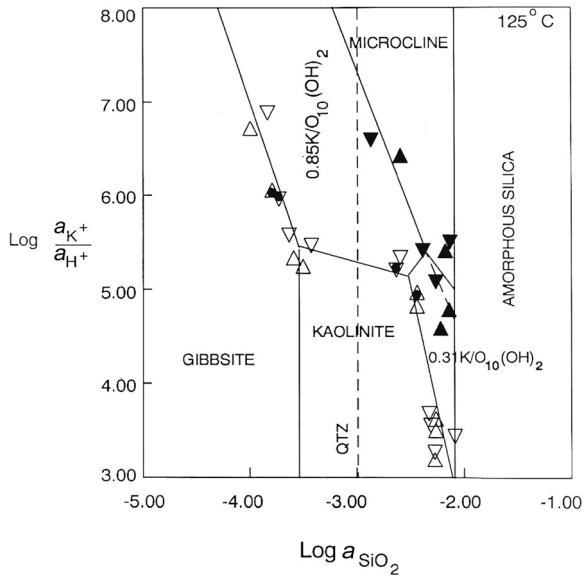

Fig. 4 Isothermal, isobaric activity diagram depicting results of solution equilibration investigations at 125°C. Open (2.0 M KC1 solutions) and partially open (0.2 M solutions) triangles show excess kaolinite; solid triangles, excess microcline (Aja et al. 1991a).

adsorption of alkali and alkaline earth cations on mineral surfaces are dominated by outer-sphere mechanisms and are, therefore, strongly dependent on ionic strength.

The dominant divalent octahedral cation in MH is Mg^{2+} (see Table 1); hence, illite equilibrium relationships were evaluated within the K_2O-MgO-SiO_2-Al_2O_3-H_2O system. In this quinary system, the composition of the solubility-controlling phases may be referred to the muscovite–MgAl celadonite [K(Al, Mg)$Si_4O_{10}(OH)_2$]–pyrophyllite compositional space and, hence, the general formula $K_x(Al_{2-y}Mg_y)(Al_{x-y}Si_{4-x+y})O_{10}(OH)_2$ (Aja et al. 1991b). Consequently, the illite ⇌ kaolinite equilibrium reaction becomes:

$$K_x\left(Al_{2-y}Mg_y\right)\left(Al_{x-y}Si_{4-x+y}\right)O_{10}(OH)_2 + (x+2y)H^+_{(aq)} + \frac{(2+x-6y)}{2}\,H_2O \rightleftharpoons xK^+_{(aq)} + yMg^{2+}_{(aq)} + (2-2x+3y)SiO_{2(aq)} + \frac{(2+x-2y)}{2}\,Al_2Si_2O_5(OH)_4 \quad (11)$$

for which the corresponding equilibrium constant expression is

$$\log\frac{a_{K^+}}{a_{H^+}} = \frac{(2x-2-3y)}{x}\log a_{SiO_{2(aq)}} - \frac{y}{x}\log\frac{a^{0.5}_{Mg^{2+}}}{a_{H^+}} + \frac{1}{x}\log K_{11} \quad (12)$$

The strong collinearity of the solubility data precluded solution of Eq. 12 directly by muliple regression analyses and, thus, a semi-empirical approach was adopted (Aja et al. 1991b). Based on the two models (Eqs 9 and 11), the compositions of the solubility-controlling phases were subsequently determined to be $K_{0.29}(Mg_{0.26}Al_{1.74})(Al_{0.03}S_{3.97})O_{10}(OH)_2$, $K_{0.50}(Mg_{0.22}Al_{1.78})(Al_{0.28}Si_{3.72})O_{10}(OH)_2$, $K_{0.69}(Mg_{0.16}Al_{1.84})(Al_{0.53}Si_{3.47})O_{10}(OH)_2$, and $K_{0.85}(Mg_{0.12}Al_{1.88})(Al_{0.73}Si_{3.27})O_{10}(OH)_2$. Standard state thermodynamic properties for these phases have also been retrieved from the solubility data (Aja 1995).

The resolution of the solubility data into linear univariant boundaries (Figs 1 and 4) implies that each solubility-limiting phase behaved as discrete phases of fixed compositions in the experimental systems. But in natural environments, the compositions of analogous phases may exhibit temporal and spatial variations. Therefore, using Gibbs energy-minimization techniques, Kulik & Aja (1997) modeled the compositional and thermodynamic data from the solution equilibration experiments (Aja 1995; Yates 1993) presuming the ternary muscovite–celadonite–pyrophyllite solid solution. Hence, the formalism:

$$\begin{aligned} G^\circ_{x,y} = {} & G^\circ_{Prl}X_{Prl} + G^\circ_{Cel}X_{Cel} + G^\circ_{Ms}X_{Ms} \\ & + RT[X_{Prl}\ln X_{Prl} + X_{Cel}\ln X_{Cel} + X_{Ms}\ln X_{Ms}] \\ & + W_{Prl\text{–}Cel}X_{Prl}X_{Cel} + W_{Prl\text{–}Ms}X_{Prl}X_{Ms} \\ & + W_{Cel\text{–}Ms}X_{Cel}X_{Ms} \\ & + W_{Prl\text{–}Cel\text{–}Ms}X_{Prl}X_{Cel}X_{Ms} \end{aligned} \quad (13)$$

In Eq. 13, $G^\circ_{x,y}$, G°_{Prl}, G°_{Cel}, G°_{Ms}, X_i, and W_i represent the Gibbs free energy of formation of the solubility controlling phases, Gibbs free energy of formation of pyrophyllite, Gibbs free energy of formation of celadonite, Gibbs free energy of formation of muscovite, mole fraction of the various endmember components, and the various Margules interaction parameters. The use of macroscopic micas in Eq. 13 reflects the non-existence of thermochemical properties of endmember clay minerals suitable for modeling the properties of illite and illitic phases. Certainly, this will affect the magnitudes of the Margules interaction parameters which exhibited no particular dependence on temperature (Table 2 in Kulik & Aja 1997); Fig. 5 depicts the variation of the calculated excess Gibbs energy at 25°C.

In the studies with natural illites summarized above, the compositions of the solubility-controlling phases were not presumed to be the same as the composition of the starting illite based on bulk chemical analyses. Thus, errors inherent in earlier solubility studies resulting from the presence of multiple phases in these natural samples were circumvented. However, a possible criticism of these studies is that the concentrations of Al in the equilibrated solutions were not determined but were presumed to have been conserved in the solid phases; this practice reflected the widely held view of the geochemical immobility of aluminum and was adopted in other studies (e.g. Hemley 1959). Perhaps, the most severe limitation of this group of solution equilibration studies was the lack of simultaneous verification, by analytical transmission electron microscopy (ATEM), of the structure and chemical compositions of the solubility-controlling phases.

Solution equilibration studies of sericite and muscovite

In further investigations of illite equilibria in the system K_2O-Al_2O_3-SiO_2-H_2O, Yates & Rosenberg (1996, 1997,

https://doi.org/10.1007/s42860-019-00044-x Published online by Cambridge University Press

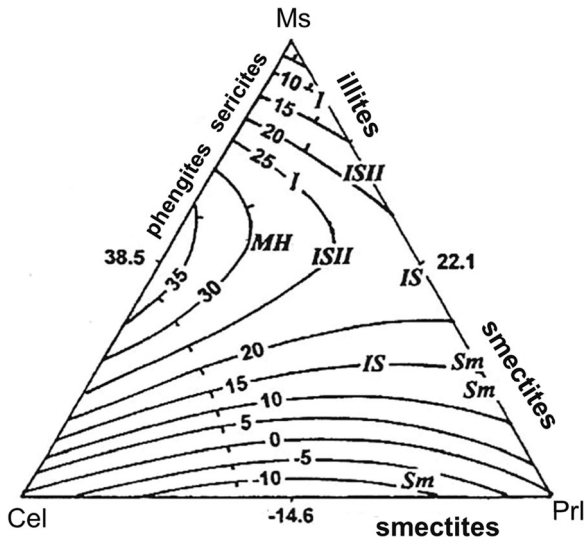

Fig. 5 Excess Gibbs energy of mixing (G^{xs}_{298}, kJ/mol) for pyrophyllite (Prl)–celadonite (Cel)–muscovite (Ms) ternary solid solution model of solubility-controlling phases; MH, bulk composition of Marblehead illite (Kulik & Aja 1997).

1998) applied the same solution equilibration techniques as were used by Sass et al. (1987) and Aja et al. (1991a); but, in lieu of natural illites, the starting materials used by them were San Juan sericites (RM30, SG4; Eberl et al. 1987) and some natural muscovites, and their investigations were conducted between 100 and 250°C. These latter studies yielded solubility-controlling phases having the approximate compositions [$K_x/O_{10}(OH)_2$] of 0.28±0.04, 0.51±0.04, and 0.88 ±0.04; in other words, the solubility-controlling phases in these latter studies were identical to those inferred from the prior studies with natural illites (Fig. 2). However, in these studies with sericites and muscovites, a phase having the approximate composition $K_{0.69}/O_{10}(OH)_2$ was not observed, probably because the experiments were conducted outside its stability field (Fig. 3).

In order to characterize better the identity of the inferred solubility-controlling phases, Yates & Rosenberg (1997) conducted solid-equilibration experiments. In solid-equilibration experiments, identical solid materials (to those used in prior solution-equilibration experiments) were reacted with aqueous solutions the compositions of which were the same as the final composition of the prior solution-equilibration experiments; however, a high solution-to-solid ratio (~120:1) was used which ensured that the solution composition did not change while the solids were brought to equilibrium with the solution. The solid products from these solid-equilibration experiments with sericites and muscovites were characterized by ATEM (Yates & Rosenberg 1997, 1998). At 250°C, neoformed illite laths grew on muscovite edges and may have resulted from dissolution of both kaolinite and muscovite edges (figs 2 and 3 in Yates & Rosenberg 1997; figs 3 and 4 in Yates & Rosenberg 1998). The neoformed illite crystals had a compositional range varying from 0.31 to 0.89 $K/O_{10}(OH)_2$; with increased duration of the experiments, the K content converged towards 0.88 $K/O_{10}(OH)_2$ which was the K content calculated from slopes of univariant boundaries in solution-equilibration experiments. The range and convergence of the illite compositions documented under isothermal conditions (Yates & Rosenberg 1988) may be indicative of crystal growth following nucleation. Nonetheless, the ATEM data appear to validate the congruence between the composition of the solubility-controlling phases inferred from slopes of univariant boundaries in ion activity diagrams and the composition of the neoformed illites. Of particular relevance to this review is the observation (Yates & Rosenberg 1996, 1997) that muscovite did not come to equilibrium in muscovite + kaolinite or muscovite + microcline solution-equilibration experiments; rather, neoformed illitic phases identical to phases observed in experiments with natural illites + kaolinite or sericites + kaolinite were the stable phases (see Fig. 6).

The attainment of equilibrium in solubility experiments such as discussed above may, therefore, be presumed if: (1) the same steady-state conditions defined in terms of the equilibrating aqueous solution compositions can be approached from both under- and over-saturation as was the case in the studies discussed above; (2) the slopes of univariant lines representing mineral-solution equilibria are rational over a wide range of solution compositions at a given temperature; and (3) results are reproducible in experiments of long duration and with a variety of analogous but different starting materials. These conditions were apparently met in the solubility studies discussed above and, thus, strongly suggest that illites and sericites may dissolve to points of thermodynamic equilibrium in solution equilibration experiments.

Solution equilibration studies of chlorites Similar solution-equilibration techniques to those employed in studies with illites, sericites, and muscovites have also been applied to the investigation of the hydrothermal stability of several chlorites (Aja & Small 1999; Aja 2002; Aja & Dyar 2002); the chlorites included a low-Fe clinochlore (or ferroan clinochlore) and two magnesian chamosites. In the studies with natural chlorites as starting materials, the solid products were examined by both X-ray diffraction and ATEM and these did not document the formation of new chlorite phases in the run products; therefore, the solubility-controlling phases were the same as the starting chlorites. In addition, the equilibrated solutions were analyzed exhaustively including for Al and trace metals and, thus, the presumption of conservation of Al in the solid phases was not necessary; ion speciation modeling of the reacted aqueous solutions were executed using EQ3/6 (Wolery 1993).

The solutions from the hydrothermal experiments with chlorites, when plotted on ion activity diagrams, resolved into univariant boundaries (Fig. 7a, b) for the experiments conducted at $T \leq 175$°C. But at 200°C (Fig. 7c), the data converged to a common point defining the kaolinite-diaspore-chlorite invariant point. These experiments were multiple batch runs having identical starting charges; the primary variable in the data plotted on Fig. 7 was the equilibrating temperature. Hence, such a transition from a univariant equilibrium to an invariant one caused solely

https://doi.org/10.1007/s42860-019-00044-x Published online by Cambridge University Press

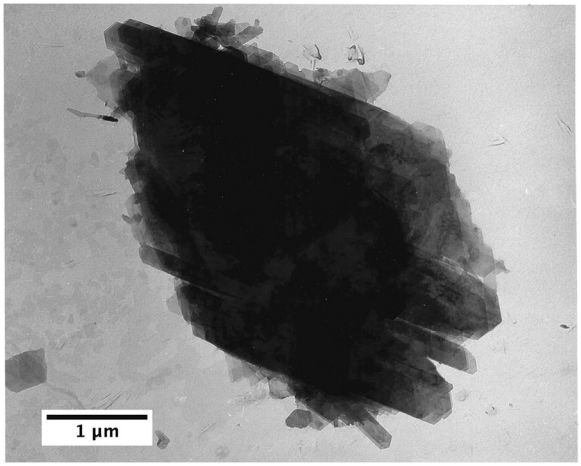

Fig. 6 TEM image of of muscovite grains with neoformed illite laths on muscovite edges. The illite grew in muscovite-kaolinite solid equilibration experiments conducted at 250°C and at saturation vapor pressure by Yates (1993).

by increasing temperatures is clearly equilibrium driven, consistent with Duhem's Law and strongly suggests the attainment of stable equilibrium in these low-temperature ($T \leq 250$°C) hydrothermal experiments. Furthermore, the multi-phase solubility documented in studies with illite-bearing assemblages was not observed in these experiments with chlorites; perhaps, this intrinsic difference in the solubility behaviors of chlorite-bearing assemblages vis-à-vis illite/sericite-bearing assemblages is rooted in differences in the nature of the interlayer material between the 2:1 layers.

DISCUSSION

In the literature, muscovite is still very commonly used as a proxy for illite in low-temperature chemical potential diagrams and this largely reflects persistent questions as to whether complex clay minerals (such as illite) are stable, metastable, or even unstable phases. Questions on the stability vs metastability of illite and related phases have revolved around three main issues: (1) are the solubility behaviors of these minerals in hydrothermal solutions amenable to treatment by the laws of equilibrium thermodynamics? (2) do illite and illite-smectite have defined stability fields relative to muscovite and pyrophyllite stability? and (3) are illites and smectites constrained to be thermodynamically metastable owing to physicochemical conditions of their environments of formation?

Models of Illite Metastability

A postulate of the metastable model of compositionally complex clay asserts that illite is metastable relative to muscovite + pyrophyllite inasmuch as a large solvus is required to explain the apparent coexistence of muscovite and pyrophyllite inferred in transmission electron microscopic investigations of metapelites from Witwatersrand and northeastern Pennsylvania (Jiang et al. 1990); they inferred that the coexistence of the muscovite and pyrophyllite resulted from the prograde decomposition of illite that had formed metastably in the muscovite-pyrophyllite solvus. By contrast, Loucks (1991) reasoned that the argument by Jiang et al. (1990) for illite metastability is false because the presumption that pyrophyllite lamella exsolved from illite is untenable considering that pyrophyllite is not a significant molecular component of illite crystalline solutions. Moreover, the compositional vector along the $Al_2Si_4O_{10}(OH)_2 \rightleftharpoons KAl_2AlSi_3O_{10}(OH)_2$ compositional trend is not a significant component of the substitutional variations of structurally bound H_2O in potassic white micas when viewed as a function of the molar proportion of conventional interlayer cations; hence, the muscovite–pyrophyllite binary is not a simple binary solvus (akin to the paragonite–muscovite solvus) but rather contains the subsidiary muscovite-hydromica and muscovite-hydropyrophyllite solid solutions (Loucks 1991). Secondly, a *T–X* stability diagram calculated for the hydrous muscovite–pyrophyllite binary (fig. 10a in Vidal & Dubacq 2009) precludes the coexistence of muscovite and pyrophyllite; rather between 275–350°C, 200–275°C, and 100–200°C, the following assemblages illite + pyrophyllite, illite + kaolinite + quartz, and illite + beidellite become successively stable, respectively; muscovite + pyrophyllite was not a stable assemblage under these conditions. Furthermore, Dubacq et al. (2011) demonstrated through Monte Carlo simulations of energetics of muscovite-pyrophyllite solid solutions, that the conclusions of the solid-state study of Jiang et al. (1990) is probably erroneous inasmuch as the stabilizing influence of hydration on clay minerals was neglected; they concluded that it is impossible to use the muscovite–pyrophyllite solvus as proof of metastability of illite as the compositions of illitic materials cannot be modeled in this system without considering the effects of hydration.

Another postulate of the metastable model of illite is that clay minerals sequences encountered during illitization reactions reflect the operation of the Ostwald step rule in which kinetic factors rather than approach to equilibrium drives illitization reactions (Essene & Peacor 1995). At the time of this postulate by Essene & Peacor (1995), the Ostwald step rule was still a theoretical conjecture; however, this is no longer the case. Using high-resolution electron microscopy, Chung et al. (2009) provided the first empirical confirmation of the Ostwald step rule more than a century after it was postulated by Ostwald (1897); they observed the ephemeral metastable crystal structures postulated by the Ostwald step rule in the formation of amorphous $LiFePO_4$ and its recrystallization to the stable (olivine) phase via the formation of a number of different metastable nanocrystal forms at 450°C. In this validation of the Ostwald step rule (Chung et al. 2009), the nucleation and crystallization occurred in a closed system under isochemical and isothermal conditions. These conditions are divergent from those under which illitization reactions occur and, hence, the notion of illite metastability predicated on the presumptive application of Ostwald's step rule to illitization reactions is questionable. Furthermore, because the presumption of Ostwald ripening during illitization reactions has been based on indirect evidence anchored on the interpretation of particle-size

https://doi.org/10.1007/s42860-019-00044-x Published online by Cambridge University Press

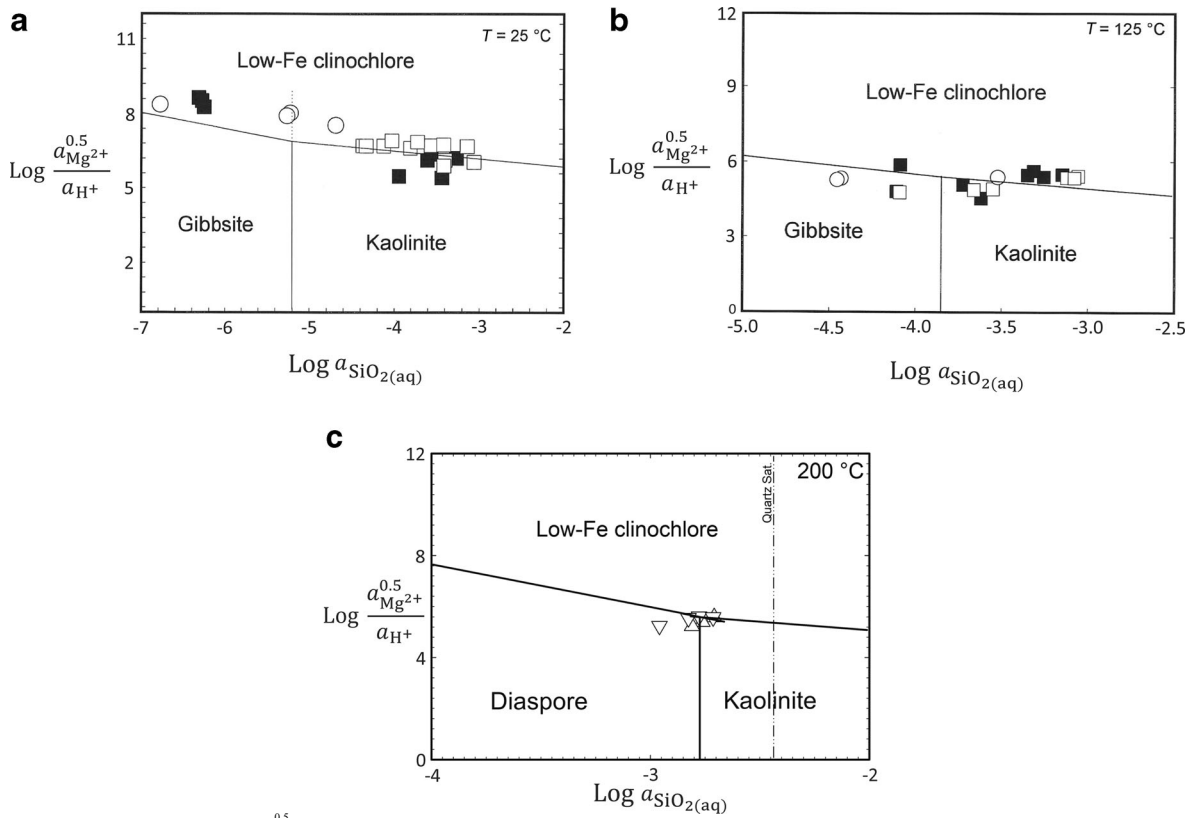

Fig. 7 Isothermal, isobaric log $\frac{a^{0.5}_{Mg^{2+}}}{a_{H^+}}$ vs log$a_{SiO_{2(aq)}}$ diagrams depicting experimental data obtained at 25°C (a), 125°C (b) and 200°C. The open circles represent experiments in which chlorite were reacted with gibbsite in aqueous NaCl solutions; open and solid squares represent experiments in which chlorite was reacted with kaolinite in the presence of aqueous $MgCl_2$ and NaCl solutions, respectively (Aja & Small 1999). Triangles denote experiments conducted in aqueous $MgCl_2$ solutions and the apices of triangles indicate direction of approach (Aja & Dyar 2002).

distribution normalized to modes, it is fraught with difficulties. As was discussed previously, earlier presumptions of the applicability of an Ostwald-type process to the sequential appearance of various phases during smectite illitization reactions now appear questionable. Moreover, the correct interpretation of Ostwald processes emphasizes structural chemistry rather than entropy production (Morse & Casey 1988) but, because the preponderance of evidence has now shown that crystal-size distributions of particles that have undergone illitization have log-normal distributions (e.g. Kim & Peacor 2002) which are rooted in maximum entropy effects, the metastability of illite cannot be presumed justifiable on the applicability of Ostwald ripening mechanisms.

The question as to whether clay minerals dissolve to points of thermodynamic equilibrium in solubility measurements dates back to Lippmann (1977, 1982) who proposed that compositionally complex clay minerals are metastable and/or disequilibrium solids and, thus, their solubility behaviors are not amenable to the law of mass action. The issues raised by Lippmann (1977, 1982) regarding the solubility characteristics of clay minerals have been treated extensively heretofore (Aja & Rosenberg 1992; Aja & Dyar 2002). Furthermore, in the series of investigations discussed in the previous section, only one smectite, one illite, and two I-S phases (Fig. 2) were found to control solubility in the presence of gibbsite/diaspore ± kaolinite or in the presence of microcline despite the differences in the chemical composition and structure of the various illites, sericites, and muscovites used as starting materials. Furthermore, the failure of muscovite to equilibrate in muscovite-bearing experiments and the neoformation of illitic phases in lieu of muscovite suggests equilibrium reversal of the stability of illite, especially considering that the compositions of the neoformed illites in experiments starting with muscovite were akin to those observed in experiments starting with natural illites of different compositions.

H_3O^+ in Illite Interlayers

The question of the state and roles of structurally bound water in illitic clays recently has been of renewed interest. On the basis of a study of SH, Nieto et al. (2010) reasoned that illite is a dioctahedral mica characterized by the exchange vector, $K_{-1}H_3O^+$, rather than by the substitution towards pyrophyllite ($SiAl_{-1}$, K_{-1}); in developing this model, they fixed the sum of tetrahedral and octahedral cations a priori to six during crystallochemical recalculation of chemical analyses. This echoes the earlier model of Brown & Norrish (1952) in which the excess H_2O found in illite is attributed to occupancy of the interlayer site by mostly K^+ and hydronium (H_3O^+) ions.

https://doi.org/10.1007/s42860-019-00044-x Published online by Cambridge University Press

This model had been deemed unsatisfactory (Hower & Mowatt 1966) inasmuch as two monomineralic illites having no expandable layers yielded chemical analyses amenable to structural recalculation of oxide composition without recourse to hydronium ions in the interlayer. The excess water in SH is more likely to occur as H_2O rather than H_3O^+ inasmuch as reasonable estimates of equilibrium conditions and water content are obtained with thermobarometric models incorporating H_2O in the interlayer position of illite (Vidal et al. 2010), and unrealistically acidic conditions are required for significant incorporation of H_3O^+ into the interlayer of illite. Indeed, the solution equilibration data at 25°C (Fig. 1a) does not support illite formation in rather acidic conditions as would be expected if H_3O^+ is a significant interlayer component.

The substitutional model of Nieto et al. (2010) essentially defaults to the muscovite ⇌ hydromica substitution of Loucks (1991) who modeled compositional variations in white micas and illites using muscovite ⇌ hydropyrophyllite $[(H_2O)Al_2Si_4O_{10}(OH)_2]$ and muscovite ⇌ hydromica $(H_3O^+)Al_2AlSi_3O_{10}(OH)_2$ substitutions. Hence, the binary solid solution, $Al_2Si_4O_{10}(OH)_2 \rightleftharpoons KAl_2AlSi_3O_{10}(OH)_2$, may not be used to model illite compositional variations; this contradicts the presumption that excess H_2O in the interlayer of illite is H_2O rather than hydronium ion (Hower & Mowatt 1966). Because excess H_2O (relative to micas) is characteristic of illites and mixed-layered I-S (Hower & Mowatt 1966), the extent of the proposed hydropyrophyllite ⇌ muscovite and hydromica ⇌ muscovite substitutions in the compositional variations of illite and I-S clay minerals needs to be spectroscopically resolved, and given the multiphase nature of SH and other reference illites (Table 1), resolution of this question requires the use of clearly monomineralic samples the bulk chemical analyses of which can be recalculated satisfactorily into a single structural formula. Obviously, the states of structurally bound water have thermochemical ramifications. For instance, the inclusion of structurally bound water in the illite general formula (Eq. 9) is not likely to affect significantly the magnitude of the slopes of the univariant phase boundaries if hydronium ion is not a component in the interlayer site (as noted previously). However, structurally bound water, even in the absence of hydronium ions, will likely have pronounced entropic effects during crystallization especially for phases with lower interlayer K-contents (e.g. smectites and I-S).

Multiphase Solubility of Illite and I-S

In the solution equilibration studies discussed previously, only a limited number of solubility-limiting phases were observed despite the wide diversity in the chemistry and mineralogy of the starting materials (Table 1) used in these studies. In addition, in non-equilibrium experiments in which sodic feldspar was reacted with aqueous KCl solutions at 150–200°C, Primmer et al. (1993) documented the neoformation of illites. Although these experiments were not designed as equilibrium experiments, the resulting aqueous solutions resolved into univariant boundaries, in $\log\frac{a_{K^+}}{a_{H^+}}$ vs $\log a_{SiO_{2(aq)}}$ ion activity space, such that the composition of the neoformed illites $[K_x/O_{10}(OH)_2]$ inferred from the univariant boundaries (using Eqs 9, 10 above) were 0.29, 0.51, and 0.87. These are clearly identical to those inferred from experiments with illites and sericites. Furthermore, ATEM analyses of the neoformed illites by Primmer et al. (1993) yielded compositions 0.27, 0.55, and 0.87 which confirmed the values they inferred from slopes of the univariant boundaries. In other words, these authigenesis experiments in which neither illite nor muscovite was used as a starting material seem to validate the results of the prior solution-equilibration experiments conducted with natural illites, sericites, and muscovite.

A multiphase illite solubility model had been proposed by Rosenberg et al. (1990) based on compositions inferred from the solution-equilibration investigations. In the multiphase model, the compositions of solubility-controlling phases observed in experiments with K-saturated Goose Lake illite, $K_{0.25}/O_{10}(OH)_2$ (Rosenberg et al. 1985) was presumed to represent K-saturated smectite whereas the phase with composition $K_{0.85}/O_{10}(OH)_2$ observed in experiments with Marblehead illite (Aja 1989) was presumed to represent end-member illite [or Illite (I)]; then the intermediate compositions $K_{0.50}/O_{10}(OH)_2$ and $K_{0.69}/O_{10}(OH)_2$ correspond closely to those expected for phases with IS $[K_{0.55}/O_{10}(OH)_2]$ and ISII $[K_{0.70}/O_{10}(OH)_2]$ ordering, respectively. In this model, the four mica-like solubility-controlling phases having the following interlayer K-contents per half unit cell 0.29 ± 0.04, 0.50 ± 0.05, 0.69 ± 0.08, and 0.85 ± 0.05, correspond then to the four layer types S, IS, ISII, and I recognized in natural I-S samples by X-ray diffractometry (Fig. 2).

The repeated appearances of these discrete phases in these experimental systems suggest the existence of certain free energy minima within illite compositional space and seem consistent with the lack of continuously ordered I-S interstratifications going from smectite-rich clays to illite-rich clays. In an X-ray diffractometry (XRD) study of expandability of 41 clays from several diagenetic settings, Środoń (1984) demonstrated a continuous variation of illite-smectite interstratifications from random, through incomplete IS to IS, incomplete ISII to ISII type of ordering; however, the existence of IIS-type of ordering was not detected in the diagenetic materials. That is, these XRD studies (Środoń 1984) documented only the existence of IS- and ISII-ordered interstratifications. The existence of only these two ordered I-S phases would seem to validate the solution equilibration data, but questions as to how many ordered I-S phases exist in different geological settings are unresolved. In a study of the smectite illitization sequence in the hydrothermally altered silicic volcanic glass in the Shinzan hydrothermal area, Inoue et al. (1987) reported the existence of R1, R2, and $R \geq 3$ ordering interstratifications. On the other hand, Dong et al. (1997), in a transmission electron microscope (TEM) investigation of five diagenetic samples, concluded that smectite, R1 IS (i.e. I-S with 50% I), and illite are the three dominant phases observed within a diagenetic sequence; according to Dong et al. (1997), R1 IS is relatively abundant whereas other kinds of mixed-layer I-S phases are rare. Clearly, the existence of a limited number of ordered interstratifications would concur with the existence of certain free-energy minima between smectite and endmember illite

https://doi.org/10.1007/s42860-019-00044-x Published online by Cambridge University Press

implied by the multiphase solubility model. However, the number of ordered interstratifications existing in different geological systems and determined using different techniques (XRD vs TEM) is not conclusive.

The relative stabilities of the solubility-controlling phases are influenced by the chemistry of coexisting pore water and temperature. In the quaternary system and at quartz saturation, stability fields are defined for only Illite (0.69K) at $T \leq 100°C$ and Illite (I) at $100°C < T < 250°C$ (Fig. 3). But in the quinary K_2O-MgO-Al_2O_3-SiO_2-H_2O system, on the other hand, smectite (0.29K) stability fields persist at quartz saturation alongside Illite (0.69K) and Illite (I) (Fig. 8). This effect of temperature and porewater chemistry on the relative stability finds empirical validation in the direct crystallization of smectite, ordered I-S, and illite from hydrothermal solutions (Tillick et al. 2001). The path towards the crystallization of endmember illite is, therefore, not unique but will depend on both the lithogeochemistry and aqueous geochemistry of the hosting environment; smectite or IS will transform directly to endmember illite given the appropriate physicochemical conditions (fig. 2 in Aja et al. 1991a; Fig. 1 in Yates & Rosenberg 1996).

The successive transformation of these solubility-controlling phases as would be expected during illitization is at odds with the presumption of Ostwald ripening as a driving force of illitization. The solubility-controlling phases are discrete thermodynamic phases having different chemistries and particle thicknesses and include smectite (S), endmember illite [Illite (I)], and the ordered interstratifications R1 (IS) and R3 (ISII). Thus, in going from smectite to Illite (I), these phases are characterized by progressively increasing interlayer K-contents and thicknesses. Being that Ostwald ripening is an isochemical process, the successive nucleation and growth of the different phases as would be expected during diagenesis and/or hydrothermal alteration would violate its basic tenets (cf. Primmer 1994). Nonetheless, Ostwald ripening may occur within the stability field of an illite phase. For instance, a phase such as endmember illite or Illite (I) may crystallize and undergo Ostwald ripening given its wide stability field (Fig. 3); in the Paris basin (Lanson & Champion 1991), illites having hexagonal morphology and interlayer charge of ~ –0.9 [that is, Illite (I)] appeared to have undergone some coarsening but during this coarsening it did not undergo compositional changes as is expected during Ostwald ripening.

Illite Stability during Diagenesis/Hydrothermal Alteration

The solution-equilibration studies summarized above have important implications for the stability of illite, especially when viewed in terms of relevant mineral paragenetic sequences. Consider, for instance, the behavior of clay minerals documented (McDowell & Elders 1980) in the Salton Sea Geothermal Field (SSGF). First, as noted by the authors, the phases described as authigenic sericite are analogous to sedimentary illite in arenaceous formations. In the SSGF, illite (sericite) and coarse-grained muscovite are not coeval in *P-T-X* stability range though some overlap occurs (fig. 2 in McDowell & Elders 1980); with increasing temperatures, illitization reactions proceeded toward ideal muscovite through phengitic substitutions. Macroscopic muscovite occurs at

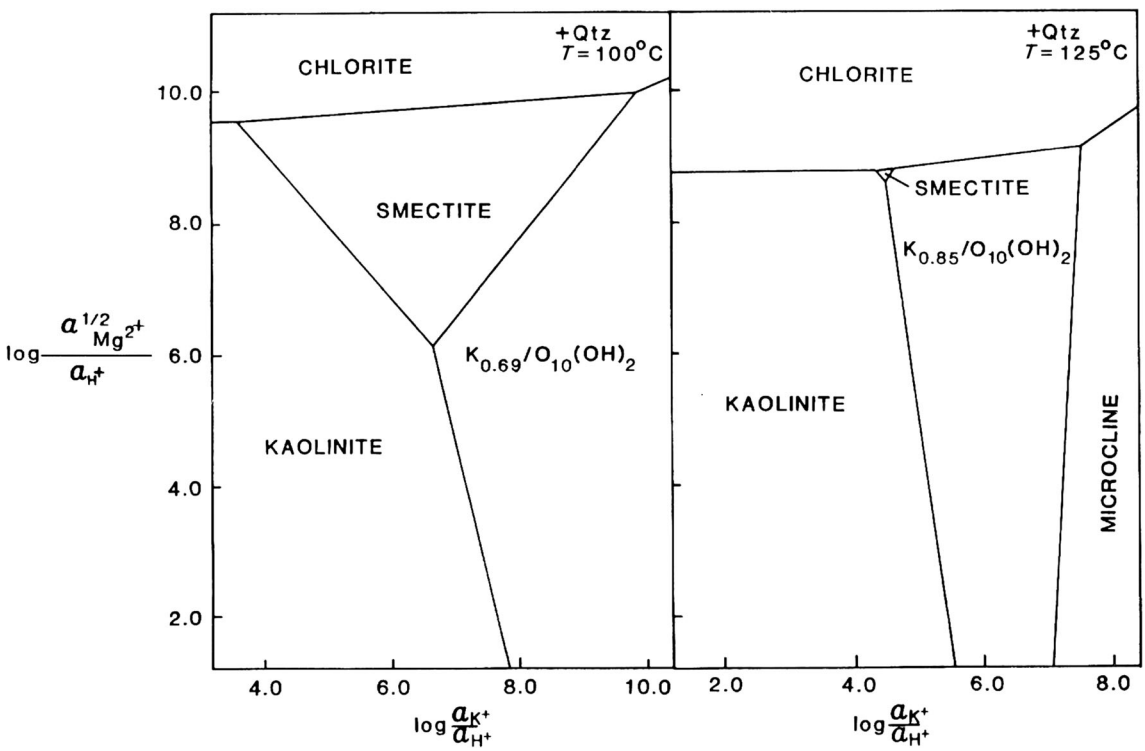

Fig. 8 Stability diagrams showing phase relationships in the system K_2O-MgO-Al_2O_3-SiO_2-H_2O in the presence of quartz at 100 and 125°C (Aja et al. 1991b).

https://doi.org/10.1007/s42860-019-00044-x Published online by Cambridge University Press

higher temperatures ($T \geq 275$°C) compared to fine-grained sericite which occurs mostly as a lower-temperature phase. At the lower temperature regimes, extensive alterations of detrital muscovite to sericites occur and conversely with increasing temperatures these sericites recrystallize to coarse-grained euhedral phengites. In addition, very fine-grained authigenic illites-sericites recrystallize to coarse-grained euhedral grains. By contrast, both authigenic fine-grained chlorites and macroscopic chlorites coexist for most of the depth range in which chlorite is stable but at ~300°C the recrystallization of the authigenic chlorites to euhedral grains also occurs along with the recrystallization of other minerals such as quartz and feldspars.

This pattern is somewhat mirrored in the experimental observations. In experiments with illite, sericite, and muscovite conducted at $25 \leq T \leq 250$°C, muscovite was not a solubility-controlling phase (Figs 2 and 3). By contrast, under comparable conditions ($25 \leq T \leq 200$°C) chlorite was shown to be stable across the low-temperature regions in which the experiments were conducted (Fig. 7). Chlorite is a structurally far more complex aluminosilicate than muscovite and would have been expected not to equilibrate with kaolinite under these conditions, but it did; whereas muscovite failed to come to equilibrium. Not only did muscovite fail to equilibrate, illite grew from the muscovite-kaolinite mixtures and came to equilibrium with kaolinite. Thus, muscovite appears to be unstable at $T \leq 250$°C and at these lower temperatures a variety of illitic phases exist and their fields of stabilities are determined by temperature and composition of coexisting aqueous solutions (Figs 3, 8). Clearly, the behaviors of illite, chlorite, and muscovite in the hydrothermal experiments seem to be borne out by the SSGF paragenesis and this buttresses the notion that clay minerals can and do dissolve to the point of thermodynamic equilibrium. Of course, the experimental stability studies were all conducted in well defined, closed experimental systems whereas clay minerals equilibria in natural systems occur under open systems subject to variable physicochemical and hydrothermal fluxes.

The SSGF paragenesis is remarkable for another reason. At temperatures near 300°C, significant recrystallization of layer silicates occurred; unaltered detrital muscovites completely recrystallized to idioblastic phengite grains and, simultaneously, aggregates of authigenic illite recrystallize to phengite mica through the process of gradual alignment and coalescence of grains. In other words, at and above this temperature, several crystallization pathways come into play for the crystallization of coarse mica; the driving force for the crystallization of macroscopic mica is sufficiently strong that alignment and coalescence of grains becomes a crystallization mechanism for authigenic illites that had persisted to this depth. Similarly, Kuwahara & Uehara (2008) in a study of the growth of hydrothermal illites reported that coalescence of particles occurred in late-stage growth and at higher temperatures compared to growth by spiral-type mechanisms. In general, crystal growth by coalescence of particles proceeds by oriented attachment of the particles during which the interface is eliminated (Li et al. 2012). In other words, structural factors that may induce strain, and possibly disorder, at the coalescing grain boundary did not preclude success of such crystal growth mechanisms and in fact are eliminated at the appropriate crystallization temperatures which reflects the magnitude of the driving force for crystallization.

The structural characteristics of illite may be thought of as the small particle-size effect of ordinary dioctahedral mica (White & Zelazny 1988). Despite this structural similarity, evidence is currently lacking for the thermodynamic stability of muscovite in the *P-T-X* regime in which illite (sericite) appears to be the stable phase. In other words, muscovite persists metastably at low temperatures ($T \leq 275$°C) but begins to crystallize at slightly higher temperature (300°C). Hence, the small size of clay minerals may have more to do with environmental factors inasmuch as at high enough temperatures ($T \approx 300$°C), idioblastic mica does form from authigenic illite by coalescence of crystallites.

A Framework for Modeling Illite and I-S Minerals

Given that muscovite is not stable in the low-temperature environment in which illites and I-S form, the wide-spread presumption that these fine-grained phases are metastable precursors of coarse-grained micas is vitiated. That is, if muscovite is not a stable phase under the conditions in which illite forms, then illite cannot be its metastable precursor. For the Ostwald step rule to apply, a macroscopic equivalent of illite must exist that would form under the same physicochemical conditions but is hindered by kinetic restrictions. Otherwise, the application of the Ostwald step rule to the stepwise smectite illitization sequence is merely presumptive. In geothermal and/or hydrothermally altered assemblages, smectite, ordered I-S, and illite crystallized directly from hydrothermal solutions without undergoing the stepwise transformation typical of illitization reactions (Tillick et al. 2001 and references therein); that is, at the appropriate temperatures and pore water chemistries, these minerals could crystallize directly without going through stepwise transformation. This is consistent with these phases having their own stability fields and agrees with the conclusions of the solution equilibration experiments (Figs 3 and 8). Hence, the stepwise transformation characteristic of the smectite illitization sequence may be documenting the transitions between phases having different stability fields rather than being a manifestation of the Ostwald step rule. Certainly, petrographic observations of illitization may be complicated by factors such as the effect of fluid/rock ratios and the role of biotic vs abiotic factors. In fact, the simultaneous operation of both abiotic and biotic controls on illitization reactions in a given geologic setting (as evident in the Nankai Trough, offshore Japan) may lead to a geologic record divergent from that resulting solely from abiotic illitization. Thus, the lack of universality in the types of ordered I-S phases encountered during illitization, as discussed previously, may be a reflection of local physicochemical conditions rather than an intrinsic metastability. In that case, geological occurrences of illite and I-S that defy current understanding must find alternate explanations other than presumptive metastability. The foregoing does not preclude these phases from

https://doi.org/10.1007/s42860-019-00044-x Published online by Cambridge University Press

being metastable. Owing to their small crystal sizes, illite and I-S phases may be treated as metastable phases inasmuch as the total Gibbs free energy of systems containing these clay minerals may not be at a minimum. Metastability derived from these considerations implies that constraints (cf. Anderson 2002) such as temperature, variable states of structural water, and the rate of entropy production may be the controlling factors. In other words, illite and related minerals are constrained to be metastable by the conditions of their formation. Nonetheless, they are thermodynamic phases the relative stability fields of which are resolvable by application of equilibrium thermodynamics.

In general, equilibrium thermodynamics has provided the framework for thinking about mineral assemblages and paragenesis, but an inherent limitation of equilibrium thermodynamics is that it deals primarily with initial and final states. Nonetheless, the starting consideration in placing the results of the hydrothermal experiments within the context of the illitization phenomenon in various geological settings should be that equilibrium thermodynamics governed the formation and stability of the different phases (i.e. smectite, IS, ISII, Illite(I)); these experiments were conducted in closed systems under isothermal conditions at the corresponding saturation vapor pressures. Furthermore, the multiphase solubility characteristic of illite-bearing systems was observed in both equilibrium (Aja et al. 1991a, 1991b; Yates & Rosenberg 1996) and non-equilibrium (Primmer et al. 1993) hydrothermal experimental systems. During prograde illitization and sedimentary basin evolution, the successive conversion of natural equivalents of these discrete phases from phases of lower to phases of increased layer charges and particle thicknesses consists of stepwise irreversible reactions. These mineralogical changes during illitization are usually accompanied by temperature and pressure changes, fluid flow, and mass transfer in the evolving sedimentary basin or hydrothermal system. Therefore, the framework of irreversible thermodynamics may provide the ideal framework to model illitization phenomena. Conceivably, in natural systems undergoing diagenesis and/or hydrothermal alteration, the discrete solubility-controlling phases (observed in solution-equilibration experiments) may be held to define boundary conditions of local equilibrium, and as the sedimentary basin/hydrothermal system evolves, the intensive variables defining equilibrium become functions of both time (t) and position (x). Because the intensive variables are continuous functions of space coordinates, the total rate of entropy production in such natural systems will be expected to conform to the model,

$$\frac{\mathrm{d}S}{\mathrm{d}t} = \int \sigma\,(x,t)\mathrm{d}V \tag{14}$$

where σ is the rate of entropy production per unit volume (V) and is given by,

$$\sigma\,(x,t) = \sum_i F_i J_i \geq 0 \tag{15}$$

where F_i is thermodynamic force driving the associated fluxes, J_i, and the inequality is an expression of the Second Law. The thermodynamic forces and fluxes in Eq. 15 will suffice to describe the system thermodynamically. In the absence of mechanical disequilibrium in the system, the forces and fluxes devolve to chemical affinities and reaction rates, and for a system with a heterogeneous distribution of temperature and chemical affinity, heat and mass transfer must be factored in with the chemical reactions (Morse & Casey 1988; Kondepudi & Prigogine 1998).

CONCLUSIONS

The basic premises of the metastability of illite have not been borne out by available data: (1) presumptions of illite metastability by projecting illite crystalline solutions onto the muscovite-pyrophyllite solvus is flawed because the stabilizing effect of hydration on illite has been omitted; (2) the extent of applicability of Ostwald processes to illitization reactions is unresolved and, therefore, cannot provide prima facie evidence for illite metastability; and (3) solution equilibration studies with illite, sericites, and chlorites confirm that clay minerals do dissolve to points of thermodynamic equilibrium in low-temperature hydrothermal solutions.

In comparative, low-temperature hydrothermal experiments with muscovite-kaolinite and chlorite-kaolinite assemblages, equilibrium was demonstrated in the latter but not in the former. In the former experiments, Illite (I) rather than muscovite equilibrated, suggesting that muscovite is not stable under these conditions. Furthermore, the combined results of hydrothermal studies conducted by several investigators with one natural muscovite and six different natural illites of contrasting lithogeochemistry (SH, GL, BB, MH, SG4, RM30) showed that only four mica-like solubility-controlling phases were observed repeatedly. These results in conjunction with mineral paragenesis from the SSGF suggest that muscovite persists metastably in *P-T* conditions in which illite/sericite forms. Thus, using muscovite as a thermodynamic proxy for illite precludes development of an accurate and rigorous model of illite stability in diagenetic and hydrothermal environments.

Morphometric studies of clays undergoing illitization have log-normal crystal-size distributions which ostensibly derive from maximum entropy effects during crystallization. Given that the correct interpretation of Ostwald processes emphasizes structural chemistry rather than entropy production and entropy production appears to be a significant factor in the formation and stability of illite, the use of Ostwald processes as an index of metastability to rationalize the sequence of clay mineralizations encountered during illitization reactions may be flawed.

ACKNOWLEDGMENTS

This work was not directly funded by any external funding agencies. Constructive and thoughtful review comments provided by the Editor-in-chief, the Associate Editor, and two journal reviewers are gratefully acknowledged. Also, the author gratefully acknowledge Dr. D. M. Yates for providing the TEM micrograph.

Compliance with Ethical Standards

Conflict of Interest

The author declares that he has no conflict of interest.

https://doi.org/10.1007/s42860-019-00044-x Published online by Cambridge University Press

REFERENCES

Ahn, J. H., & Peacor, D. R. (1986). Transmission and analytical electron microscopy of the smectite-to-illite transition. *Clays and Clay Minerals, 34*, 165–179.

Aja, S. U. (1989) A hydrothermal study of illite stability relationships between 25 and 250°C and $P_v = P_{H_2O}$. PhD thesis, Washington State University.

Aja, S. U. (1991). Illite equilibria in solutions: III. A reinterpretation of the data of Sass et al. (1987). *Geochimica et Cosmochimica Acta, 55*, 3431–3435.

Aja, S. U. (1995). Thermodynamic properties of some 2:1 layer clay minerals from solution-equilibration data. *European Journal of Mineralogy, 7*, 325–333.

Aja, S. U. (2002). The stability of Fe-Mg chlorites in hydrothermal solutions: II. Thermodynamic properties. *Clays and Clay Minerals, 50*, 591–600.

Aja, S. U., & Dyar, M. D. (2002). The stability of Fe-Mg chlorites in hydrothermal solutions I. Results of experimental investigations. *Applied Geochemistry, 17*, 1219–1239.

Aja, S. U., & Rosenberg, P. E. (1992). The thermodynamic status of compositionally-variable clay minerals: A discussion. *Clays and Clay Minerals, 40*, 292–299.

Aja, S. U., & Rosenberg, P. E. (1996). The thermodynamic status of compositionally-complex clay minerals: Discussion of "Clay Mineral thermometry – A critical perspective". *Clays and Clay Minerals, 44*, 560–568.

Aja, S. U., Rosenberg, P. E., & Kittrick, J. A. (1991a). Illite equilibria in solutions: I. Phase relationships in the system K_2O-Al_2O_3-SiO_2-H_2O between 25 and 250°C. *Geochimica et Cosmochimica Acta, 55*, 1353–1364.

Aja, S. U., Rosenberg, P. E., & Kittrick, J. A. (1991b). Illite equilibria in solutions: II. Phase relationships in the system K_2O-Al_2O_3-MgO-SiO_2-H_2O. *Geochimica et Cosmochimica Acta, 55*, 1365–1374.

Aja, S.U., & Small, J.S. (1999) The solubility of a low-Fe clinochlore between 25 and 175°C and $P_v = P_{H_2O}$ *European Journal of Mineralogy*, *11*, 829–842.

Altaner, S. P., & Ylagan, R. F. (1997). Comparison of structural models of mixed-layer illite/smectite and reaction mechanisms of smectite illitization. *Clays and Clay Minerals, 45*, 517–533.

Anderson, G. M. (2002) Stable and metastable equilibrium: the third constraint. In R. Hellman, & S. A. Wood. (eds), *Water-Rock Interactions, Ore Deposits, and Environmental Geochemistry: a Tribute to David A. Crerar* (pp. 181–189). The Geochemical Society, Special Publications, 7.

Baldan, A. (2002). Review Progress in Ostwald ripening theories and their applications to nickel-base superalloys Part I: Ostwald ripening theories. *Journal of Materials Science, 37*, 2171–2202.

Berrill, J. B., & Davis, R. O. (1980). Maximum entropy and the magnitude distribution. *Bulletin of the Seismological Society of America, 70*, 1823–1831.

Boles, J. R., & Franks, S. G. (1979). Clay diagenesis in Wilcox sandstones of Southwest Texas: implications of smectite diagenesis on sandstone cementation. *Journal of Sedimentary Petrology, 49*, 55–70.

Brown, G., & Norrish, K. (1952). Hydrous micas. *Mineralogical Magazine, 29*, 929–932.

Chung, S.-Y., Kim, Y.-M., Kim, J.-G., & Kim, Y.-J. (2009). Multiphase transformation and Ostwald's rule of stages during crystallization of a metal phosphate. *Nature Physics, 5*, 68–73.

De Yoreo, J. J., & Vekilov, P. G. (2003). Principles of crystal nucleation and growth. *Reviews in Mineralogy, 54*, 57–93.

Dong, H., & Peacor, D. R. (1996). TEM observations of coherent stacking relations in smectite, IIS and illite of shales: evidence for MacEwan crystallites and dominance of $2M_1$ polytypism. *Clays and Clay Minerals, 44*, 257–275.

Dong, H., Peacor, D. R., & Freed, R. L. (1997). Phase relations among smectite, R1 illite-smectite, and illite. *American Mineralogist, 82*, 379–391.

Drits, V. A., Lindgreen, H., Sakharov, B. A., Jakobsen, H. J., Fallick, A. F., Salyn, A. I., Dainyk, I. G., Zviagina, B. B., & Barfod, D. N. (2007). Formation and transformation of mixed-layer minerals by Tertiary intrusives in Cretaceous mudstones, West Greenland. *Clays and Clay Minerals, 55*, 260–283.

Dubacq, D., Vidal, O., & Lewin, É. (2011). Atomistic investigation of the pyrophyllite substitution and implications on clay stability. *American Mineralogist, 96*, 241–249.

Dunoyer de Segonzac, G. (1970). The transformation of clay minerals during diagenesis and low-grade metamorphism: a review. *Sedimentology, 15*, 281–346.

Eberl, D. D., & Hower, J. (1977). The hydrothermal transformation of sodium and potassium smectite into mixed layer clay. *Clays and Clay Minerals, 28*, 161–172.

Eberl, D. D., Środoń, J., Lee, M., Nadeau, P. H., & Northrop, H. R. (1987). Sericite from the Silverton caldera, Colorado: Correlation among structure, composition, origin, and particle thickness. *American Mineralogist, 72*, 914–934.

Eberl, D. D., & Środoń, J. (1988). Ostwald ripening and interparticle diffraction effects for illite crystals. *American Mineralogist, 73*, 1335–1345.

Eberl, D. D., Środoń, J., Kralik, M., Taylor, B., & Peterman, Z. E. (1990). Ostwald ripening of clays and metamorphic minerals. *Science, 248*, 474–477.

Eberl, D. D., Drits, V. A., & Środoń, J. (1998). Deducing growth mechanisms for minerals from the shapes of crystal size distributions. *American Journal of Science, 298*, 499–533.

Essene, E. J., & Peacor, D. R. (1995). Clay mineral thermometry: A critical perspective. *Clays and Clay Minerals, 43*, 540–553.

Foscolos, A. E., & Kodama, H. (1974). Diagenesis of clay minerals from Lower Cretaceous shales of North Eastern British Columbia. *Clays and Clay Minerals, 22*, 319–335.

Gailhanou, H., Blanc, P., Rogez, J., Mikaelian, G., Kawaji, H., Olives, J., Amouric, M., Denoyel, R., Bourrelly, S., Montouillout, V., Viellard, P., Fialips, C. I., Michau, N., & Gaucher, E. C. (2012). Thermodynamic properties of illite, smectite and beidellite by calorimetric methods: Enthalpies of formation, heat capacities, entropies and Gibbs free energies of formation. *Geochimica et Cosmochimica Acta, 89*, 279–391.

Garrels, R. M., & Howard, P. (1957). Reactions of feldspar and mica with water at low temperature and pressure. *Clays and Clay Minerals, 6*, 68–88.

Gaudette, H. E. (1965). Illite from Fond du Lac County, Wisconsin. *American Mineralogist, 50*, 411–417.

Gaudette, H. E., Eades, J. L., & Grim, R. E. (1966a). The nature of illites. *Clays and Clay Minerals, 13*, 33–48.

Gaudette, H. E., Grim, R. E., & Metzger, C. F. (1966b). Illite: a model based on the sorption behavior of cesium. *American Mineralogist, 51*, 1649–1656.

Grim, R. E., & Bradley, W. F. (1939). A unique clay from the Goose Lake, Illinois, area. *Journal of American Ceramic Society, 22*, 157–164.

Grim, R. E., Bray, R. H., & Bradley, W. F. (1937). The mica in argillaceous sediments. *American Mineralogist, 22*, 813–829.

Groṅholm, T., & Annila, A. (2007). Natural distribution. *Mathematical Biosciences, 210*, 659–667.

Güven, N. (1972). Electron optical observations in Marblehead illite. *Clays and Clay Minerals, 37*, 1–11.

Hartman, P. (1973). Structure and morphology. In P. Hartman (Ed.), *Crystal Growth: an Introduction* (pp. 358–402). Amsterdam: North Holland Publishing Company.

Heling, D. (1974). Diagenetic alteration of smectite in argillaceous sediments of the Rhinegraben. *Sedimentology, 21*, 463–472.

Hemley, J. J. (1959). Some mineralogic equilibria in the system K_2O-Al_2O_3-SiO_2 -H_2O. *American Journal of Science, 57*, 241–270.

Hower, J., & Mowatt, T. C. (1966). The mineralogy of illites and mixed-layer illite-montmorillonites. *American Mineralogist, 51*, 825–854.

Hower, J., Eslinger, E. V., Hower, M. E., & Perry, E. A. (1976). Mechanism of burial metamorphism of argillaceous sediments: 1.

https://doi.org/10.1007/s42860-019-00044-x Published online by Cambridge University Press

Mineralogical and chemical evidence. Geological Society of America Bulletin, 87, 725–737.

Inoue, A. (1983). Potassium fixation by clay minerals during hydrothermal treatment. *Clays and Clay Minerals, 31*, 81–91.

Inoue, A., & Kitagawa, R. (1994). Morphological characteristics of illitic clay minerals from a hydrothermal system. *American Mineralogist, 79*, 700–711.

Inoue, A., & Utada, M. (1983). Further investigations of a conversion series of dioctahedral mica/smectites in the Shinzan hydrothermal alteration area, northeast Japan. *Clays and Clay Minerals, 31*, 401–412.

Inoue, A., Minto, H., & Utada, M. (1978). Mineralogical properties and occurrence of illite/montmorillonite mixed layer minerals formed from Miocene volcanic glass in Waga-Omono district. *Clay Science, 5*, 123–136.

Inoue, A., Kohyama, N., Kitagawa, R., & Watanabe, T. (1987). Chemical and morphological evidence for the conversion of smectite to illite. *Clays and Clay Minerals, 35*, 111–120.

Inoue, A., Velde, B., Meunier, A., & Touchard, G. (1988). Mechanism of illite formation during smectite-to-illite conversion in a hydrothermal system. *American Mineralogist, 73*, 1325–1334.

Jaisi, D. P., Eberl, D. D., Dong, H., & Kim, J. (2011). The formation of illite from nontronite by mesophilic and thermophilic bacterial reaction. *Clays and Clay Minerals, 59*, 21–33.

Jiang, W., Essene, E. J., & Peacor, D. R. (1990). Transmission electron microscopic study of coexisting pyrophyllite and muscovite: direct evidence for the metastability of illite. *Clays and Clay Minerals, 38*, 225–240.

Kittrick, J. A. (1984). Solubility measurements of phases in three illites. *Clays and Clay Minerals, 32*, 115–124.

Kim, J., & Peacor, D. R. (2002). Crystal-size distributions of clays during episodic diagenesis: The Salton Sea geothermal system. *Clays and Clay Minerals, 50*, 371–380.

Kim, J., Dong, H., Seabaugh, J., Newell, S., & Eberl, D. D. (2004). Role of microbes in the smectite-to-illite reaction. *Science, 303*, 830–832.

Kim, J., Dong, H., Yang, K., Park, H., Elliott, W. C., Spivack, A., Koo, T.-H., Kim, G., Morono, Y., Henkel, S., Inagaki, F., Zeng, Q., Hoshino, T., & Heuer, V. B. (2019). Naturally occurring, microbially induced smectite-to-illite reaction. *Geology, 47*, 535–539.

Kondepudi, D., & Prigogine, I. (1998). *Modern Thermodynamics: From Heat Engines to Dissipative Structures*. New York: John Wiley.

Kuila, U., & Prasad, M. (2013). Specific surface area and pore-size distribution in clays and shales. *Geophysical Prospecting, 61*, 341–362.

Kulik, D. A., & Aja, S. U. (1997). The hydrothermal stability of illite: implications of empirical correlations and Gibbs energy minimization. In D. A. Palmer & D. J. Wesolowski (Eds.), *Proceedings of the Fifth International Symposium on Hydrothermal Reactions* (pp. 288–292). Gatlinburg, Tennessee, USA: ORNL.

Kuwahara, Y., & Uehara, S. (2008). AFM study on surface microtopography, morphology and crystal growth of hydrothermal illite in Izumiyama pottery stone from Arita, Saga Prefecture, Japan. *The Open Mineralogy Journal, 2*, 34–37.

Lanson, B., & Champion, D. (1991). The I/S-to-illite reaction in the late stage diagenesis. *American Journal of Science, 291*, 473–506.

Li, D., Nielsen, M. H., Lee, J. R. I., Frandsen, C., Banfield, J. F., & De Yoreo, J. J. (2012). Direction-specific interactions control crystal growth by oriented attachment. *Science, 336*, 1014–1018.

Lifshitz, I. M., & Slyozov, V. V. (1961). The kinetics of precipitation from supersaturated solid solutions. *Journal of Physics and Chemistry of Solids, 19*, 35–50.

Lippmann, F. (1977). The solubility product of complex minerals, mixed-crystals and three-layer clay minerals. *Neues Jahrbuch für Mineralogie – Abhandlungen, 130*, 243–263.

Lippmann, F. (1982). The thermodynamic status of clay minerals. In H. van Olphen & F. Veniale (Eds.), *Proceedings of the 7th International Clay Conference Bologna, Pavia 1981* (pp. 475–485). New York: Elsevier.

Lonker, S. W., Fitz Gerald, J. D., Hedenquist, J. W., & Walshe, J. (1990). Mineral-fluid interactions in the Broadlands-Ohaaki geothermal system, New Zealand. *American Journal of Science, 290*, 995–1068.

Loucks, R. R. (1991). The bound interlayer H_2O content of potassic white micas: muscovite-hydromuscovite-hydropyrophyllite solutions. *American Mineralogist, 76*, 1563–1579.

Manning, D. A. C. (2003). Experimental studies of mineral occurrences. In R. H. Worden & S. Morad (Eds.), *Clay Mineral Cements in Sandstones* (pp. 177–190). Oxford: International Association of Sedimentologists Special Publications 34, Blackwell Publishing company.

Mankin, C. J., & Dodd, C. G. (1963). Proposed reference illite from the Ouchita Mountains of Southeastern Oklahoma. *Clays and Clay Minerals, 10*, 372–379.

McDowell, D. S., & Elders, W. A. (1980). Authigenic layer silicate minerals in borehole Elmore 1, Salton Sea Geothermal Field, California, USA. *Contributions to Mineralogy and Petrology, 74*, 293–310.

Meunier, A. (2006). Why are clay minerals small? *Clay Minerals, 41*, 551–566.

Montoya, J. W., & Hemley, J. J. (1975). Activity relations and stabilities in alkali feldspar and mica alteration reactions. *Economic Geology, 70*, 577–594.

Morse, J. W., & Casey, W. H. (1988). Ostwald processes and mineral paragenesis in sediments. *American Journal of Science, 288*, 537–560.

Muffler, P. L. J., & White, D. E. (1969). Active metamorphism of Upper Cenozoic sediments in the Salton Sea geothermal field and the Salton Trough, southeastern California. *Geological Society of America Bulletin, 80*, 157–182.

Nadeau, P. H., & Reynolds Jr., R. C. (1981). Burial and contact metamorphism in the Mancos Shale. *Clays and Clay Minerals, 29*, 249–259.

Nieto, F., Mellini, M., & Abad, I. (2010). The role of H_3O^+ in the crystal structure of illite. *Clays and Clay Minerals, 58*, 238–246.

Ostwald, W. Z. (1897). Studien über die Bildung und Umwandlung fester Körper. I. Abhandlung: Ubersattigung and Uberkaltung. *Zeitschrift für Physikalische Chemie, 22*, 289–330.

Perry, E., & Hower, J. (1970). Burial diagenesis in Gulf Coast pelitic sediments. *Clays and Clay Minerals, 18*, 165–177.

Pollastro, R. M. (1985). Mineralogical and morphological evidence for the formation of illite at the expense of illite/smectite. *Clays and Clay Minerals, 33*, 265–274.

Prigogine, I. (1961). *Introduction to Thermodynamics of Irreversible Processes, 2e*. New York: Interscience Publishers–John Wiley.

Primmer, T. J. (1994). Some comments on the chemistry and stability of interstratified illite-smectite and the role of Ostwald-type processes. *Clay Minerals, 29*, 63–68.

Primmer, T. J., Warren, E. A., Sharma, B. K., & Atkins, M. P. (1993). The stability of experimental grown clay minerals: implications for modelling the stability of neoformed clay minerals. In D. A. C. Manning, P. L. Hall, & C. R. Hughes (Eds.), *Geochemistry of Clay-Pore Fluid Interactions* (pp. 163–180). London: Chapman & Hall.

Pytte, A. M., & Reynolds, R. C. (1989). The thermal transformation of smectite to illite. In N. D. Naeser & T. H. McCulloh (Eds.), *Thermal History of Sedimentary Basins* (pp. 133–140). New York, NY: Springer.

Reesman, A. L., & Keller, W. D. (1968). Aqueous solubility studies of high alumina and clay minerals. *American Mineralogist, 53*, 929–942.

Roberson, H. E., & Lahann, R. W. (1981). Smectite to illite conversion rates: effects of solution chemistry. *Clays and Clay Minerals, 29*, 129–135.

Rosenberg, P. E., Kittrick, J. A., & Sass, B. M. (1985). Implications of illite/smectite stability diagrams: A discussion. *Clays and Clay Minerals, 33*, 561–562.

Rosenberg, P. E., Kittrick, J. A., & Aja, S. U. (1990). Mixed-layer illite/smectite: A multiphase model. *American Mineralogist, 75*, 1182–1185.

Routson, R. C., & Kittrick, J. A. (1971) Illite solubility. *Proceeding of Soil Science Society of America*, *36*, 714-718.

Sass, B. M., Rosenberg, P. E., & Kittrick, J. A. (1987). The stability of illite/smectite during diagenesis: An experimental study. *Geochimica et Cosmochimica Acta, 51*, 2103–2115.

Sharma, V., & Annila, A. (2007). Natural process – natural selection. *Biophysical Chemistry, 127*, 123–128.

Smith, M. M., Dai, Z., & Caroll, S. A. (2017). Illite dissolution kinetics from 100 to 280 C and pH 3 to 9. *Geochimica et Cosmochimica Acta, 209*, 9–23.

Środoń, J. (1984). X-ray powder diffraction identification of illitic materials. *Clays and Clay Minerals, 32*, 337–349.

Środoń, J., & Eberl, D. D (1984) Illite. *Reviews in Mineralogy*, *13*, 495–544.

Środoń, J., Eberl, D. D., & Drits, V. A. (2000). Evolution of fundamental-particle size during illitization of smectite and implications for reaction mechanism. *Clays and Clay Minerals, 48*, 446–458.

Steiner, A. (1968). Clay minerals in hydrothermally altered rocks at Wairakei, New Zealand. *Clays and Clay Minerals, 16*, 193–213.

Tillick, D. A., Peacor, D. R., & Mauk, J. L. (2001). Genesis of dioctahedral phyllosilicates during hydrothermal alteration of volcanic rocks: I. the Golden Cross epithermal ore deposit, New Zealand. *Clays and Clay Minerals, 49*, 126–140.

Van Moort, J. C. (1971). A comparative study of the diagenetic alteration of clay minerals in Mesozoic shales from Papua, New Guinea, and in Tertiary shales from Louisiana, U.S.A. *Clays and Clay Minerals, 19*, 1–20.

Vidal, O., & Dubacq, B. (2009). Thermodynamic modelling of clay dehydration, stability and compositional evolution with temperature, pressure and H_2O activity. *Geochimica et Cosmochimica Acta, 73*, 6544–6564.

Vidal, O., Dubacq, B., & Lanari, P. (2010). Comment on "The role of H_3O^+ in the crystal structure of illite by F. Nieto, M. Melini, and I. Abad". *Clays and Clay Minerals, 58*, 717–720.

Wagner, C. (1961). Theorie der Alterung von Neiderschliigen durch UmItisen (Ostwald Reifung). *Zeitschrift fiir Electrochemie, 65*, 581–591.

White, G. N., & Zelazny, L. W. (1988). Analysis and implications of the edge structure of dioctahedral phyllosilicates. *Clays and Clay Minerals, 36*, 141–146.

Wolery, T. J. (1993) EQ3/6, A software package for geochemical modelling of aqueous systems (Version 7.2). Lawrence Livermore Nat. Lab. UCRL-MA 110662.

Yates, D. M. (1993) Experimental investigation of the formation and stability of endmember illite from 100 to 250°C and Pv.H_20. PhD thesis, Washington State University.

Yates, D.M., & Rosenberg, P.E. (1996) Formation and stability of endmember illite: I. Solution equilibration experiments at 100° to 150° C and $P_{v,\ soln}$. *Geochimica et Cosmochimica Acta*, *60*, 1873–1883.

Yates, D.M., & Rosenberg, P.E. (1997) Formation and stability of endmember illite: II. Solid equilibration experiments at 100 to 250°C and $P_{v,\ soln}$. *Geochimica et Cosmochimica Acta*, *61*, 3135–3144.

Yates, D. M., & Rosenberg, P. E. (1998). Characterization of neoformed illite from hydrothermal experiments at 250 8C and$P_{v,\ soln}$: An HRTEM/ATEM study. *American Mineralogist, 83*, 1199–1208.

Yau, S. -T., Petsev, D. N., Thomas, B. R., & Vekilov, P. G. (2000). Molecular-level thermodynamic and kinetic parameters for the self-assembly of apoferritin molecules into crystals. *Journal of Molecular Biology, 303*, 667–678.

Zhang, G., Kim, J., Dong, H., & Sommer, A. J. (2007). Microbial effects in promoting the smectite to illite reaction: role of organic matter intercalated in the interlayer. *American Mineralogist, 92*, 1401–1410.

[*Received 2 August 2019; revised 4 November 2019; AE: Warren D. Huff*]